



How can process-based modeling improve peat CO₂ and N₂O emission factors for oil palm plantations?



Erin Swails^{a,*}, Kristell Hergoualc'h^a, Jia Deng^b, Steve Froking^b, Nisa Novita^c

^a Center for International Forestry Research, Jalan CIFOR, Situ Gede, Sindang Barang, Bogor 16115, Indonesia

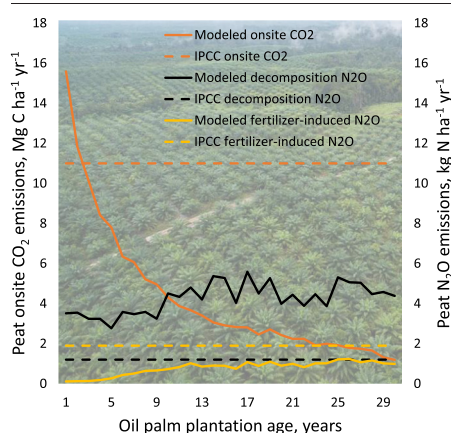
^b Earth Systems Research Center, Institute for the Study of Earth, Oceans and Space, University of New Hampshire, 8 College Road, Durham, NH 03824, USA

^c Yayasan Konservasi Alam Nusantara, Graha Iskandarsyah 3rd floor, Jalan Iskandarsyah Raya 66 C, 12160 Jakarta, Indonesia

HIGHLIGHTS

- Modeled oil palm peat GHG emissions decreased over the rotation.
- Annual GHG variations are related to precipitation, water table, soil C:N and mineral N.
- Oil palm peat GHG emission factors should consider temporal variations in emissions.

GRAPHICAL ABSTRACT



ARTICLE INFO

Editor: Wei Shi

Keywords:

Greenhouse gas (GHG) emissions
Tropical peatland
Land-use change
DNDC
Carbon dioxide
Nitrous oxide

ABSTRACT

Oil palm plantations on peat and associated drainage generate sizeable GHG emissions. Current IPCC default emission factors (EF) for oil palm on organic soil are based on a very limited number of observations from young plantations, thereby resulting in large uncertainties in emissions estimates. To explore the potential of process-based modeling to refine oil palm peat CO₂ and N₂O EFs, we simulated peat GHG emissions and biogeophysical variables over 30 years in plantations of Central Kalimantan, Indonesia. The DNDC model simulated well the magnitude of C inputs (litterfall and root mortality) and dynamics of annual heterotrophic respiration and peat decomposition N₂O fluxes. The modeled peat onsite CO₂-C EF was lower than the IPCC default (11 Mg C ha⁻¹ yr⁻¹) and decreased from 7.7 ± 0.4 Mg C ha⁻¹ yr⁻¹ in the first decade to 3.0 ± 0.2 and 1.8 ± 0.3 Mg C ha⁻¹ yr⁻¹ in the second and third decades of the rotation. The modeled N₂O-N EF from peat decomposition was higher than the IPCC default (1.2 kg N ha⁻¹ yr⁻¹) and increased from 3.5 ± 0.3 kg N ha⁻¹ yr⁻¹ in the first decade to 4.7–4.6 ± 0.5 kg N ha⁻¹ yr⁻¹ in the following ones. Modeled fertilizer-induced N₂O emissions were minimal and much less than 1.6% of N inputs recommended by the IPCC in wet climates regardless of soil type. Temporal variations in EFs were strongly linked to soil C:N ratio and soil mineral N content for CO₂ and fertilizer-induced N₂O emissions, and to precipitation, water table level and soil NH₄⁺ content for peat decomposition N₂O emissions. These results suggest that current IPCC EFs for oil palm on organic soil could over-estimate peat onsite CO₂ emissions and underestimate peat decomposition N₂O emissions and that temporal variation in emissions should be considered for further improvement of EFs.

* Corresponding author.

E-mail address: e.swails@cgiar.org (E. Swails).

1. Introduction

Tropical peatlands are an important terrestrial carbon (C) sink (Yu et al., 2010), but as a result of intensifying anthropogenic disturbance, they have become a growing source of greenhouse gas (GHG) emissions to the atmosphere (Frolking et al., 2011; Huang et al., 2021; Leifeld et al., 2019; Leifeld and Menichetti, 2018). In Southeast Asia, which holds a large proportion of global tropical peatlands (Gumbrecht et al., 2017), expansion of oil palm plantations dominates patterns of land-use change in peat swamp forests (Miettinen et al., 2012, 2016; Schoneveld et al., 2019). Conversion of peat forest to oil palm entails drainage of soils, land-clearing fires, drastic changes to vegetation cover, and fertilizer application, profoundly altering peat chemistry and transforming the ecosystem from a potential C sink to a large net GHG source (Hergoualch and Verchot, 2014; McCalmont et al., 2021; Swails et al., 2021).

When intact, peatlands are seasonally or permanently water-logged ecosystems where vegetation litter input exceeds soil organic matter (SOM) decomposition, leading to the accumulation of carbon-rich peat deposits. Conversion and drainage of peatlands accelerates aerobic peat decomposition as the result of increased oxygen availability, leading to increased CO₂ emissions from heterotrophic respiration (Hergoualch et al., 2017; Itoh et al., 2017), while changes to vegetation alter C inputs to peat from above-ground litterfall and root mortality (Hergoualch and Verchot, 2014). CH₄ emissions from anaerobic peat decomposition are decreased by peatland drainage (Hergoualch and Verchot, 2012). The impact of drainage on N₂O emissions from tropical peatlands is inconsistent, with both undrained and drained peat soils acting as a N₂O source (Pärn et al., 2018). In lands converted for agriculture, nitrogen (N) fertilization stimulates peat N₂O emissions (Chaddy et al., 2019; Oktarita et al., 2017; Sakata et al., 2015). In oil palm plantations, biogeophysical drivers of peat GHG fluxes – water table level (Chaddy et al., 2019; Melling et al., 2005), soil moisture (Chaddy et al., 2019; Manning et al., 2019; Marwanto and Agus, 2014), soil temperature (Manning et al., 2019; Oktarita et al., 2017), vegetation productivity (Hergoualch and Verchot, 2014; Swails et al., 2021), and peat chemistry (Swails et al., 2018) – vary temporally and micro-spatially according to management practice and geographic location, thus driving enormous heterogeneity in peat GHG emissions (Swails et al., 2021). Given the considerable spatio-temporal variability in peat GHG fluxes, assessment of peat GHG emissions from oil palm plantations is challenging.

Countries report their GHG emissions to the UNFCCC (United Nations Framework Convention on Climate Change) using guidelines developed by the Intergovernmental Panel on Climate Change (IPCC). The 2013 Wetland supplement provides in Chapter 2 (Drösler et al., 2014), default Tier 1 emission factors (EF) for oil palm plantations on organic soil for quantifying peat emissions of CO₂ onsite, N₂O emissions from peat decomposition, and peat CH₄ emissions. N₂O emissions from N fertilizer application are accounted for separately using national fertilizer application data regardless of soil type following the 2019 refinement of the 2006 guidelines (Hergoualch et al., 2019). The IPCC defines the onsite peat CO₂ EF as the difference between C inputs to peat from vegetation litter (the sum of aboveground litterfall and root mortality) and C outputs from aerobic decomposition of organic matter (or heterotrophic respiration). While measurements of total soil respiration are relatively straightforward, partitioning of total soil respiration into autotrophic and heterotrophic components is more difficult. Also, assessment of belowground litter inputs from root mortality is challenging. Separating N₂O emissions from peat decomposition and emissions induced by fertilizer application requires intensive and spatially stratified sampling which is laborious.

While field measurements are constrained by time and budget, process-based models offer the possibility to test hypotheses for improving EF by simulating processes that are relevant to peat GHG production and uptake. Using process-based models, EF can be simulated and simple empirical relationships between GHG emissions and drivers can be derived from modeled data. Presently, process-based modeling has been used widely in temperate (e.g., Frolking et al., 2010; Tang et al., 2010) and boreal (e.g., Deng et al., 2014; Kettunen, 2003; Rinne et al., 2018) peatlands, but

has not been applied extensively in tropical peatlands. Modeling of peat GHG fluxes in tropical settings has been constrained by scarcity of data for parameterization of soil processes and validation of modeled results. Only a small number of studies using process-based modeling in tropical peatlands have been published, and these predominantly related to long-term peat accumulation of carbon (e.g., Kurnianto et al., 2015; Warren et al., 2017) and net ecosystem productivity (e.g., Mezbahuddin et al., 2014) with limited application to peat GHG fluxes (Sa'adi et al., 2022). There is a need to test the capacity of models to simulate peat GHG emissions in tropical settings, where climate variations and peat-forming vegetation differ substantially from temperate and boreal zones (Farmer et al., 2011).

The DeNitrification and DeComposition (DNDC) model is a process-based biogeochemical model simulating ecosystem C and N dynamics that has been evaluated against field measurements of GHG fluxes from soils worldwide (Gillespy et al., 2014; Giltrap et al., 2010). The model was originally designed for simulating N₂O emission and soil organic carbon (SOC) change in upland cropping systems (Li et al., 1992; Li et al., 1994a), and has been adapted and modified for use in other ecosystems including forests, (Li et al., 2005), wetlands, (Zhang et al., 2002), northern peatlands (Deng et al., 2014, 2017), and livestock farms (Li et al., 2012). DNDC has been used to investigate agricultural GHG emissions in temperate (Taft et al., 2019) and sub-tropical (Li et al., 1994b) peats, and is particularly useful for generating GHG emissions for key tropical peatland land-use categories and management practices such as oil palm because the model can simulate impacts of common agricultural management practices on GHG emissions while also incorporating wetland hydrology (Zhang et al., 2002) and biogeochemical processes in organic soils (Li et al., 1992). In this study, we tested DNDC in oil palm plantations on peat with the goals of (1) assessing its potential to simulate dynamics of peat GHG flux and biogeophysical variables (vegetation productivity, water table level, soil water-filled pore space, and soil temperature), (2) deriving EF for peat onsite CO₂ emissions and N₂O emissions from peat decomposition and N fertilization, and testing their stability over the plantation rotation period, and (3) investigating relationships among these EF and easily measurable drivers. We focused on CO₂ and N₂O emissions, which together account for almost 100% of the peat GHG budget in oil palm plantations (Swails et al., 2021), and disregarded peat CH₄ emissions which are negligible in this system (Drösler et al., 2014).

2. Methods

2.1. Field measurements

To calibrate model parameters and validate modeled peat GHG fluxes, we used field measurements collected in a peatland on the southern coast of Indonesian Borneo in Central Kalimantan. The climate of the region is humid tropical, characterized by high annual rainfall (2719 mm, Iskandar Airport, Pangkalan Bun, 2001–2020) with a brief dry season, and average daily temperature remaining fairly constant during the year. August is, on average, the driest month (105 mm of rain). Mean annual temperature is 26.6 °C with mean monthly temperature ranging from 26.3 °C in July to 27.2 °C in May (Iskandar Airport, Pangkalan Bun, 2001–2020).

The field site was located approximately 10 km from the city of Pangkalan Bun (S 02° 49.410', E 111° 48.785') (Fig. 1a). Permanent plots were established at the site in 2012 in three smallholder oil palm plantations (OP-2007, OP-2009, and OP-2011). Land use history and land management practices are described for each plantation in the Supplementary Information (S1).

We designed our sampling approach to capture spatial and temporal heterogeneity in environmental conditions and GHG fluxes from soils. One month before beginning the study we deployed measurement equipment at six subplot locations per plot (Fig. 1b). At each subplot we installed equipment close to the base of a palm under the palm canopy (CT) and at mid-distance between two palms (FT) to capture the influence of micro-

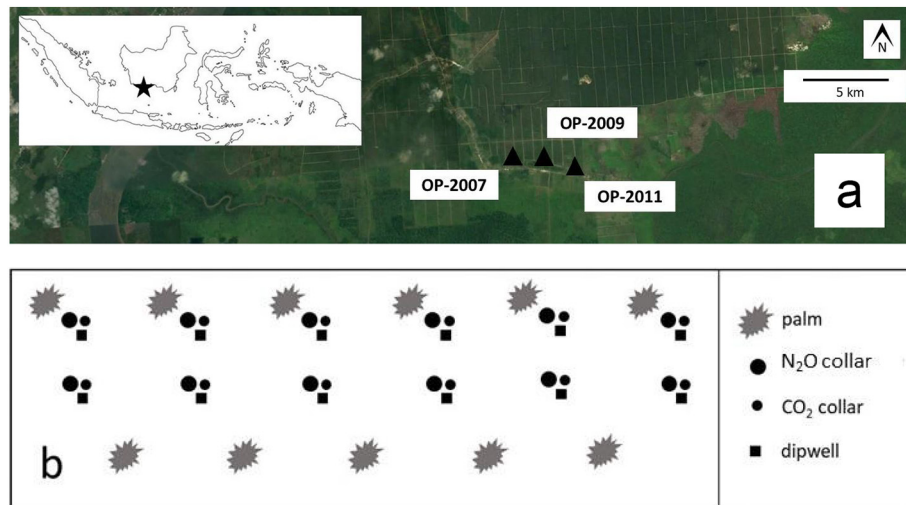


Fig. 1. Field sampling design. Measurements were collected from a peatland on the island of Indonesian Borneo in Central Kalimantan (inset, a) in three plots in smallholder oil palm plantations (OP-2007, OP-2009, OP-2011) (a). In each plot, GHG chamber collars (circles) and surface wells (squares) were installed at six subplot locations (b). At each subplot, one pair of collars and a surface well was installed at the base of a palm, and another set of collars and surface well was installed mid-distance between two palms. Palms were spaced at a distance of approximately 8–9 m in a triangular design (after Swails et al., 2021).

spatial heterogeneity in vegetation processes and management activities on peat GHG fluxes and biogeophysical drivers. The 2 m-radius area around palms (CT) is where smallholders applied fertilizers and where roots are usually most active (Nelson et al., 2006, 2015). Soil temperatures are typically higher far from palms due to the impact of canopy shading close to palms, particularly in young plantations where the canopy is not closed (Oktarita et al., 2017; Swails et al., 2019).

We measured soil N_2O fluxes monthly from September 2012 until June 2015, and once more in September 2015 when El Niño strongly reduced precipitation, with concurrent measurements of total soil respiration commencing in December 2012. Fluxes were not intensively monitored during post-fertilization periods, thus measured N_2O fluxes stem from peat decomposition and exclude short-term fertilizer-induced emissions.

Soil temperature and moisture (water-filled pore space) (WFPS) at the topsoil layer (0–5 cm) and water table level were monitored concurrently with gas fluxes at CT and FT positions from September 2012 to June 2015 and once more in September 2015. Further details on methods for measurement of soil GHG fluxes and environmental variables are provided in the Supplementary Information (S2).

Spatio-temporal variations of soil GHG fluxes and environmental variables from January 2014 to June 2015 and in September 2015 are reported by Swails et al. (2019, 2021). The Supplementary Information (S2) provides a more complete dataset covering the entire monitoring period from September 2012 to September 2015.

2.2. Modeling

2.2.1. DNDC model overview

The DNDC model consists of two components. The first component includes the soil climate, vegetation growth and decomposition sub-models. These sub-models predict daily soil temperature, moisture, pH, redox potential, CO_2 flux and substrate concentration profiles (e.g., NH_4^+ , NO_3^- , dissolved organic carbon [DOC]), based on ecological drivers (climate, soil, vegetation and anthropogenic activity). Water table level dynamics are predicted by DNDC using several parameters to estimate lateral flows, including surface inflow rate, maximum water table depths for surface and ground outflows, and surface and ground outflow rates (Zhang et al., 2002). The second component comprises the fermentation, nitrification, and denitrification sub-models. These sub-models predict daily CH_4 and N gas fluxes (NO , N_2O , N_2 , and NH_3) based on the soil environmental variables predicted by the sub-models of the first component (Li, 2000). Geochemical and biogeochemical reactions in the model have been

parameterized using laboratory and field studies in addition to classical laws of physics, chemistry, and biology (Gilhespy et al., 2014).

To model decomposition, SOM is divided into litter, humads (substances partly stabilized by humification and adsorption [McGill et al., 1981]), and humus pools representing compounds with different intrinsic decomposition rates (Li et al., 1992). The litter pool is further divided into very labile, labile, and resistant sub-pools. The actual modeled rate of SOM decomposition depends on soil clay content (minimal in organic soils) and thermal and moisture conditions as well as the size of each SOM pool and sub-pool (Li et al., 2000).

Modeled nitrification rate is regulated by soil ammonium (NH_4^+) concentration, temperature, moisture, clay content, pH, and aerobic fraction of soils (Li, 2000). Denitrification is simulated as a sequential reduction process (NO_3^- , NO_2^- , NO , N_2O , N_2), with rate regulated by concentrations of electron donor (i.e., DOC) and acceptors (i.e., N species) in the anaerobic fraction of soils (Li, 2000). The relative proportions of NO , N_2O and N_2 gases emitted depends on soil moisture and available substrates for nitrification and denitrification processes.

2.2.2. Model input data

Peat GHG fluxes and biogeophysical drivers were simulated for each of the three plantations. We used a combination of site-level (weather, vegetation, and agricultural management practices), and plot-level or sub-plot level (hydrology and soil) input values. Input parameter values were carefully selected and calibrated to simulate conditions in peat soils. Daily meteorological data, including maximum and minimum air temperatures and precipitation, were obtained from the local meteorological station at Iskandar Airport in Pangkalan Bun, 10 km from the study site. Phenological and physiological parameters related to palm growth (biomass partitioning and C:N ratio) were taken from the literature (Table S1). Management practices modeled in oil palm plots included planting, fertilizing, and harvesting. Palms were planted in the first year of simulations and N- and P-fertilized every three months following rates applied locally (S1) with application rate decreasing from 150 to 84 kg N-P $ha^{-1} yr^{-1}$ in years 1–3, to 135–76 kg N-P $ha^{-1} yr^{-1}$ in years 4–6, to 120–67 kg N-P $ha^{-1} yr^{-1}$ in years 7–30. Oil palm fruit harvest was set to occur once per month starting in year three, as typically practiced. While in situ, fronds are cut at fruit harvest, and piled in stacks between palms, aboveground litterfall occurred evenly over space and time in model simulations. Additional model inputs are described in the Supplementary Information (S3).

To account for microspatial variation in peat CO_2 and N_2O fluxes and drivers, DNDC was run separately for close to palm (CT) and far from

palm (FT) positions. To model soil respiration and biomass growth, CT simulations were performed with vegetation (oil palm) and fertilization while FT simulations were performed with no vegetation (bare peat) and no fertilization. To model N₂O emissions from peat decomposition, CT simulations were performed with vegetation but no fertilization, and FT simulations were performed as above. Information on the individual spin-up periods can be found in the Supplementary Information (S3).

2.2.3. Model calibration

Parameters for simulating vegetation growth and senescence were adjusted by comparing simulated aboveground and belowground biomass accumulation, aboveground litterfall, and root mortality to literature values. Environmental variables (water table level, soil WFPS, and soil temperature) collected from the plantations during Sep 2012 – Sep 2015 were used to calibrate additional soil (Table S2) and hydrological parameters (Table S4). Peat C:N ratio and GHG flux measurements (total soil respiration and peat decomposition N₂O) measured in situ during Sep 2012 – Aug 2013 were utilized to calibrate SOM partitioning among the model's litter, humads, and humus pools (Table S3). S3 provides additional details on model calibration.

2.2.4. Model validation

Simulated mean annual total soil respiration, heterotrophic respiration, and N₂O fluxes from peat decomposition were validated against mean annual fluxes determined from field measurements collected during Sep 2013 – Sep 2015. Spatial ratios were used to scale-up modeled and measured fluxes for CT and FT simulations to the plot level. We used the ratio of area within a 2 m radius of palms (CT) to the area outside of this radius (FT). The CT to FT ratios in oil palm plantations were 25:75 (OP-2011), 27:73 (OP-2009), and 37:63 (OP-2007) (Swails et al., 2019). Annual in situ heterotrophic respiration rate was estimated from total soil respiration using the partitioning ratios of $61.0 \pm 2.3\%$ for OP-2007 and $82.5 \pm 5.7\%$ for OP-2011, measured from Jun 2013 – Jun 2014 (over 13 months) in the two plantations (Hergoualc'h et al., 2017). An average partitioning ratio of $71.8 \pm 10.8\%$ was applied for OP-2009, considering the plantation age was between those of OP-2007 and OP-2011.

We used statistical indicators of correlation and coincidence to evaluate the overall agreement between simulated and measured values. A high correlation between simulations and measurements indicates that the model simulates the dynamics of the measured variable well, whereas a high coincidence indicates that the magnitude of the simulated values closely corresponds to the measured values (Smith et al., 1996). Pearson's correlation coefficient (r) and relative root mean squared error (RMSE) between simulated and in situ mean annual total soil respiration, heterotrophic respiration, and N₂O fluxes were used to assess correlation and coincidence, respectively. To further investigate causes for deviations between simulations and measurements, we partitioned the mean squared error ($MSE = RMSE^2$) into the sum of the squared bias ($SB = \text{squared mean deviation}$), the squared difference between standard deviations (SDSD), and the lack of correlation weighted by the standard deviations (LCS) (Koboyashi and Salam, 2000). SB represents bias of the simulation. SDSD represents the difference in the magnitude of fluctuation between the simulation and measurement, while LCS represents the correlation between simulated and measured values. A larger SDSD indicates that the model failed to simulate the magnitude of the fluctuation, while a larger LCS means that the model failed to simulate the pattern of the fluctuation.

2.2.5. Model application

To derive EF for peat onsite CO₂ emissions and N₂O emissions from peat decomposition and N fertilization, test the stability of these EF over the plantation rotation period, and investigate relationships among EF and easily measurable drivers, we ran simulations for each plantation over a 30-year period typical of oil palm rotation cycles. Model input was as for model calibration and validation, with the following changes. We input daily weather from the meteorological station at Iskandar Airport for the years 2007–2020 and assigned daily weather from a year randomly selected between 2007 and 2020 for each year thereafter (2021–2040). Fertilizer was applied

four times a year using common N application rates practiced in Southeast Asia, with plantations receiving $75 \text{ kg N ha}^{-1} \text{ yr}^{-1}$ until the palms had reached maturity at three years (Mutert et al., 1999) and $125 \text{ kg N ha}^{-1} \text{ yr}^{-1}$ thereafter (Darmosarkoro et al., 2003). To model peat CO₂ emissions, CT simulations were performed with vegetation (oil palm) and fertilization while FT simulations were performed with no vegetation (bare peat) and no fertilization. Following the IPCC guidelines (Drösler et al., 2014), the peat onsite CO₂ EF ($EF_{\text{modeled CO}_2 \text{ onsite}}$) was calculated as the difference in C outputs from heterotrophic respiration and C inputs from litterfall and root mortality. To model N₂O EF for peat decomposition ($EF_{\text{modeled N}_2\text{O decomp}}$), CT simulations were performed with vegetation but no fertilization. The EF for fertilizer-induced N₂O emissions ($EF_{\text{modeled N}_2\text{O fert}}$) was computed as the difference in N₂O emissions in simulations with and without N fertilization divided by the annual N application rate.

The mean and standard error of annual peat onsite CO₂ and N₂O EF was calculated over the 30-year rotation period ($n = 3$ plantations per year), and per decade (0–10, 10–20, 20–30 years). Error in decadal means was calculated by propagating annual EF errors ($n = 10$ years). Mean annual and decadal EF were compared to the IPCC defaults for oil palm plantation on organic soil (Drösler et al., 2014) and to in situ values from our sites. The modeled N₂O EF for N fertilization was compared to the IPCC EF for synthetic fertilizer inputs in wet climates (Hergoualc'h et al., 2019).

We investigated relationships between modeled annual EF ($EF_{\text{modeled CO}_2 \text{ onsite}}$, $EF_{\text{modeled N}_2\text{O decomp}}$ and $EF_{\text{modeled N}_2\text{O fert}}$) and annual precipitation, water table level, and soil WFPS, C:N ratio and mineral N content (NO_3^- and NH_4^+) using univariate regression and stepwise multiple linear regression with Akaike Information Criterion (AIC) for model selection. For both univariate and multiple regressions we took the average of the three plots in each year of the simulation ($n = 30$). In all cases, CT and FT simulations were scaled-up to the plot level. All statistical analyses were computed using R version 4.0.4. A threshold p value of 0.05 was used for significance.

3. Results

3.1. Model calibration

3.1.1. Vegetation

Aboveground (AGB) and belowground (BGB) oil palm biomass, aboveground litterfall, and root mortality modeled by DNDC and averaged across the three plantations are presented in Fig. 2 and compared to in situ measured results and to the literature. DNDC-modeled AGB increased over time following a trend similar to the model by Khasanah et al. (2015) for Indonesian industrial plantations on peat (Fig. 2a) and was in close agreement with in situ observations. BGB reached a plateau after 10 years and was greater than in situ BGB. For plantations older than 5 years modeled BGB was greater than BGB estimated from AGB applying the equation of Henson and Dolmat (2003) (Fig. 2b). However, the 30-year time-averaged ratio of modeled BGB to modeled AGB (0.75) was similar to the root:shoot ratio modeled by Henson and Dolmat (2003) (0.76). Aboveground litterfall also plateaued after 10 years and was within the range of litterfall rates reported in the literature and measured in situ (Fig. 2c). The 30-year-average aboveground litterfall rate modeled by DNDC was $2.6 \pm 0.1 \text{ Mg C ha}^{-1} \text{ yr}^{-1}$, slightly higher than the average rate computed from the literature ($2.1 \pm 0.2 \text{ Mg C ha}^{-1} \text{ yr}^{-1}$, $n = 12$) (Fig. 2c). Root mortality rate steadied after 20 years and was below the linear model of Henson and Dolmat (2003) for oil palm plantations on peat. DNDC predicted an average root mortality rate over a 30-year rotation of $3.9 \pm 0.2 \text{ Mg C ha}^{-1} \text{ yr}^{-1}$, slightly lower than the mean calculated from the literature ($5.0 \pm 1.0 \text{ Mg C ha}^{-1} \text{ yr}^{-1}$, $n = 5$) (Fig. 2d).

3.1.2. Hydrology and soil

Modeled and in situ water table level, soil WFPS, and soil temperature are shown in Fig. 3. The model simulated water table level and its fluctuation well overall. Lower water table levels were predicted during dry months, when total monthly precipitation was $<100 \text{ mm}$ (Sep 2012,

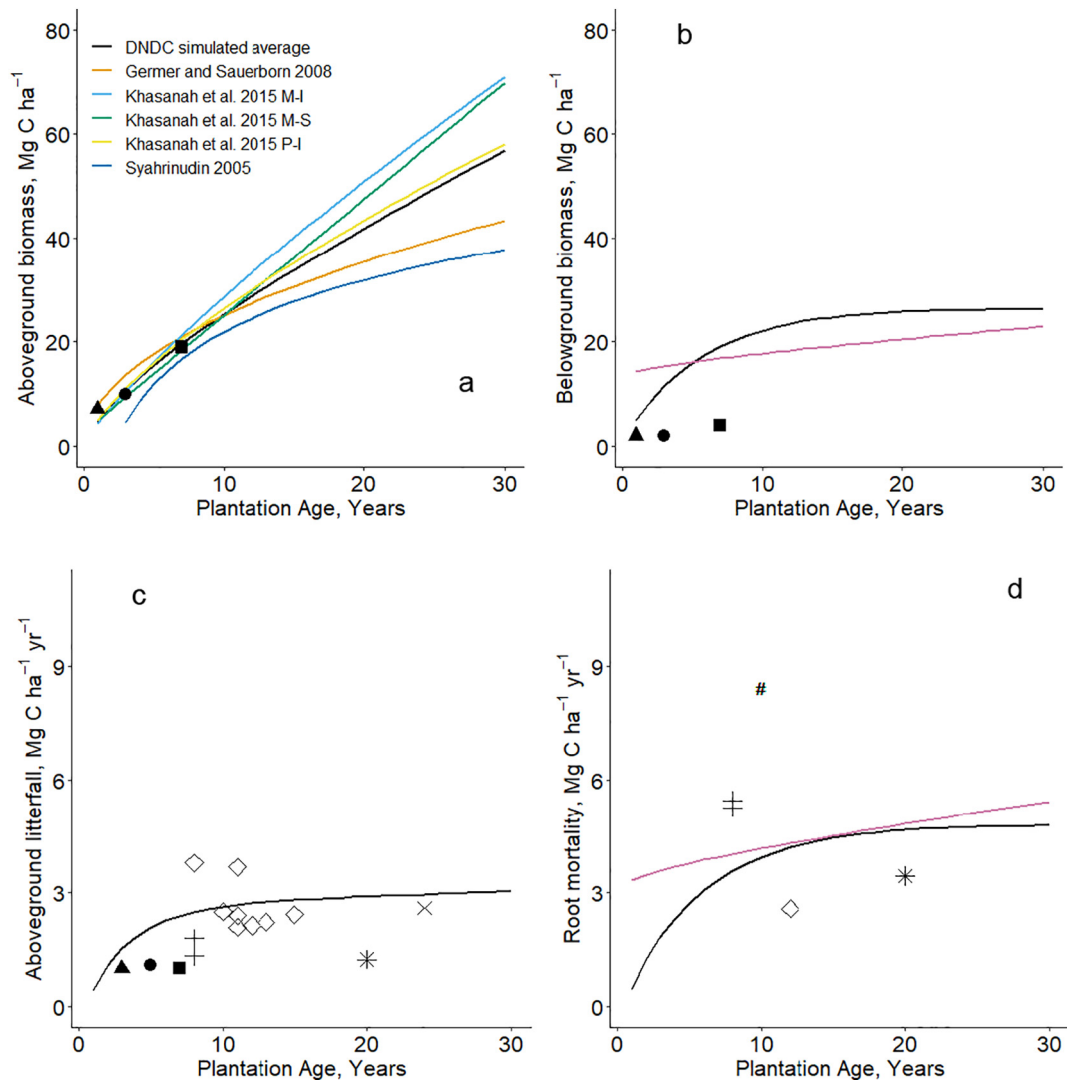


Fig. 2. Oil palm aboveground biomass (AGB) (a), belowground biomass (BGB) (b), aboveground litterfall (c), and root mortality (d) modeled in this study (black line, average of the three plantations) and reported in the literature (symbols and colored lines). In situ measured results are presented for the three plantations (OP-2011, triangle; OP-2009, circle; OP-2007, square) in (a), (b) (Novita et al., 2021), and (c) (Swails et al., 2021). Panel (a) presents AGB modeled by Germer and Sauerborn (2008) (for plantations on peat and mineral soils), by Khasanah et al. (2015) (for industrial plantations on mineral soil, M – I; for smallholder plantations on mineral soil, M – S; and for industrial plantations on peat soil, P – I), and by Syahrudin (2005) (for plantations on mineral soils). Panel (b) displays BGB modeled by Henson and Dolmat (2003) (pink line). Panel (c) presents aboveground litterfall measured by Lamade et al. (1996) (asterisk), Lamade and Setiyo (2002) (cross), Dresscher et al. (2016) (diamond), and Wakhid and Hirano (2021) (x). Panel (d) presents root mortality modeled by Henson and Dolmat (2003) (pink line) and measured by Lamade et al. (1996) (asterisk), Henson and Chai (1997) (hashtag), Lamade and Setiyo (2002) (cross), and Kotowska et al. (2016) (diamond).

Jul – Oct 2014, Jun – Sep 2015) (Fig. S1a), but the model did not accurately simulate water table levels of more than 1.5 m below the soil surface. DNDC captured the decrease in soil moisture during the dry season in 2014 and 2015 but not in 2013, when total monthly precipitation did not fall below 100 mm (Fig. S1a). Modeled soil WFPS was highly variable temporally, and generally higher far from palms than close to palms in all plots, in agreement with in situ observations (Fig. S2b). The model accurately predicted the magnitude (but not temporal variation) of observed soil temperature in OP-2009 and OP-2011. The modeled soil temperature CT and FT was generally higher than the observed soil temperature in OP-2007, indicating that the model did not simulate the influence of vegetation shading in the oldest oil palm plantation.

Modeled and in situ total soil respiration and N₂O emissions from peat decomposition during Sep 2012 – Aug 2013 (model calibration year) are displayed in Fig. 4. DNDC simulated the magnitude of total

soil respiration satisfactorily overall for both spatial positions, with total soil respiration higher close to palm than far from palm. The model presented limitations in simulating the monthly variation in mean total soil respiration, but the variation in total soil respiration was high within plots, and the simulated values were generally within one standard deviation of field observations. The mean modeled contributions of heterotrophic respiration to total soil respiration at the plot scale were 76.3% and 88.4% for OP-2007 and OP-2011, respectively, compared to $61.0 \pm 2.3\%$ and $82.5 \pm 5.7\%$ determined in situ by Hergoualc'h et al. (2017) in the same plantations.

The predicted N₂O fluxes were generally of the same magnitude as the observed N₂O fluxes in all plots, and N₂O fluxes were higher far from palm than close to palm, in agreement with field observations (Fig. S2e). Occasional N₂O uptakes observed in situ (Fig. 4), were not simulated by DNDC which does not have an algorithm to model this process. The model also

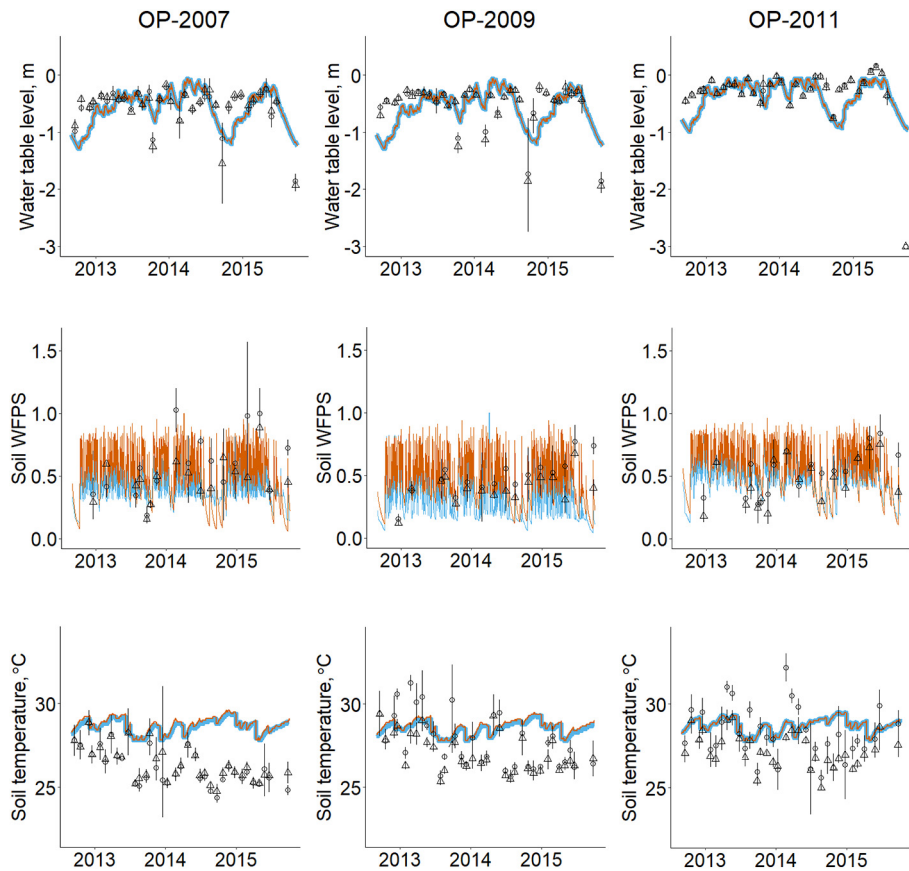


Fig. 3. Modeled daily and in situ mean monthly water table level, soil water-filled pore space (WFPS), and soil temperature during Sep 2012 – Sep 2015 in OP-2007, OP-2009, and OP-2011. The blue and red lines indicate simulated values close to palm (CT) and far from palm (FT), respectively. Measured values at CT and FT positions are respectively indicated by triangles and circles. Water table levels below the soil surface are indicated by negative values. The vertical bars indicate standard deviation of replicates ($n = 6$).

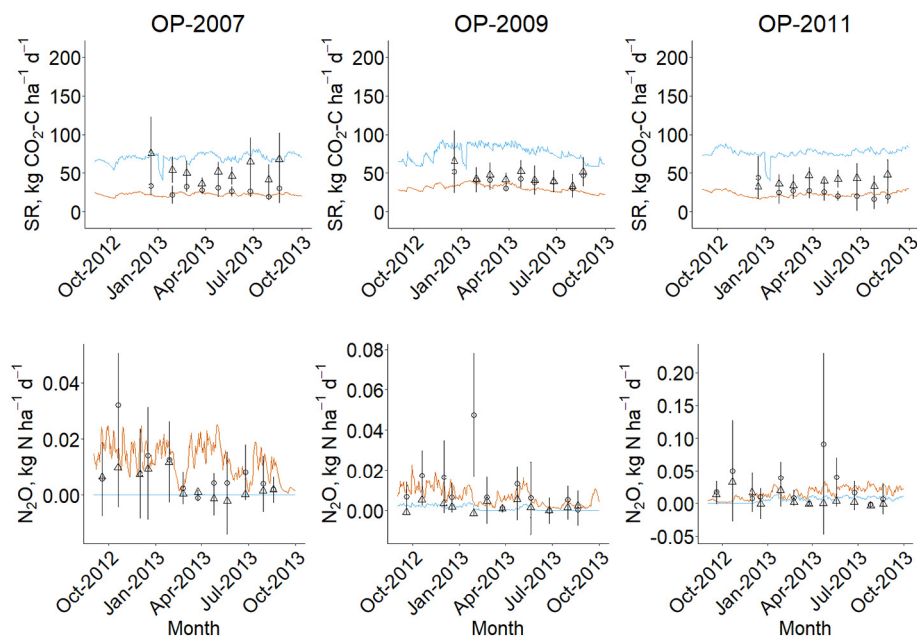


Fig. 4. Modeled daily and in situ mean monthly total soil respiration (SR) and N_2O emissions stemming from peat decomposition during Sep 2012 – Aug 2013 (model calibration year) in OP-2007, OP-2009, and OP-2011. The blue and red lines indicate simulated values close to palm (CT) and far from palm (FT), respectively. Measured values at CT and FT positions are respectively indicated by triangles and circles. The vertical bars indicate standard deviation of replicates ($n = 6$).

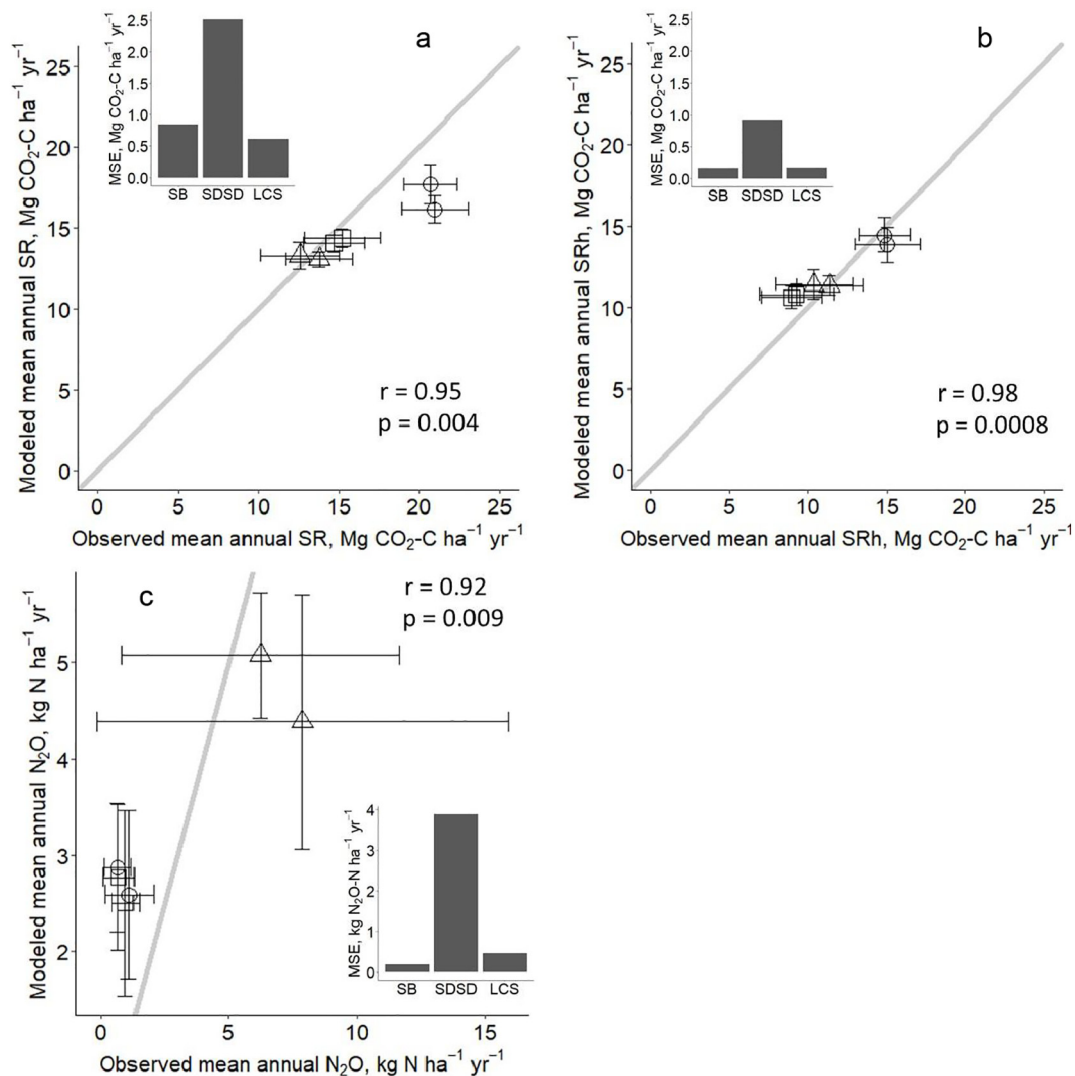


Fig. 5. Modeled and in situ total soil respiration (SR) (a), heterotrophic soil respiration (SRh) (b), and N_2O emissions stemming from peat decomposition (c) in oil palm plantations. Squares indicate OP-2007, circles OP-2009, and triangles OP-2011. Each point is the mean value per plot during approximately one year (Sep 2013 – Aug 2014 and Sep 2014 – Sep 2015) and the vertical and horizontal bar are its associated standard error. The solid line shows the 1:1 relationship. The Pearson correlation coefficient (r) and associated p value as well as the mean squared errors (MSE) between modeled and observed emissions are presented. The MSE comprises three components: the squared bias (SB), the squared difference between standard deviations (SDDS), and the lack of correlation weighted by the standard deviations (LCS). The RMSE (root mean squared error) is the square root of MSE.

did not simulate the observed pulse of N_2O that occurred at the FT position in OP-2011 (Fig. 4).

3.2. Model validation

The high Pearson correlation coefficients between modeled and observed mean annual total soil respiration, heterotrophic respiration and peat decomposition N_2O emission rates indicate that the dynamics of the annual fluxes were well simulated by DNDC over the limited number of observations from our sites (Fig. 5a, b, c). The root mean squared errors (RMSE) of mean annual total soil respiration ($2.4 \text{ Mg CO}_2\text{-C ha}^{-1} \text{ yr}^{-1}$) and heterotrophic respiration ($1.1 \text{ Mg CO}_2\text{-C ha}^{-1} \text{ yr}^{-1}$) were low and amounted to, respectively 15% and 10% of mean annual observed rates (16.3 and $11.6 \text{ Mg CO}_2\text{-C ha}^{-1} \text{ yr}^{-1}$, respectively). On the other hand, the RMSE of mean annual peat decomposition N_2O emissions ($2.1 \text{ kg N ha}^{-1} \text{ yr}^{-1}$) was 73% of the observed flux ($2.9 \text{ kg N ha}^{-1} \text{ yr}^{-1}$). For all three fluxes, the large contribution of SDDS to MSE indicates that the model did not simulate the full magnitude of fluctuation among observations (Figure 5a-c insets). Monthly variation in modeled and in situ peat GHG fluxes are presented in the Supplementary Information (S4).

3.3. Model application

3.3.1. Peat onsite CO_2 and N_2O emission factors

Mean annual and decadal modeled peat onsite CO_2 emissions ($EF_{\text{modeled } CO_2 \text{ onsite}}$) are compared with the IPCC default for oil palm plantations on organic soil ($EF_{\text{IPCC } CO_2 \text{ onsite}} = 11 \text{ Mg CO}_2 \text{ ha}^{-1} \text{ yr}^{-1}$, Dröslér et al., 2014) and in situ observations in Fig. 6a. $EF_{\text{modeled } CO_2 \text{ onsite}}$ decreased over time due to a decline of heterotrophic respiration more important than the simultaneous increase in C inputs from litterfall and root mortality over the first decade (Fig. 6b). Decreasing heterotrophic respiration was related to reduction in the modeled SOM litter pool fraction (Fig. S4). In the first decade modeled EF ($EF_{\text{modeled } CO_2 \text{ onsite } 0-10 \text{ years}} = 7.7 \pm 0.4 \text{ Mg C ha}^{-1} \text{ yr}^{-1}$) overlapped the 95% confidence interval of the IPCC default, but fell below this range in the second ($EF_{\text{modeled } CO_2 \text{ onsite } 10-20 \text{ year}} = 3.0 \pm 0.2 \text{ Mg C ha}^{-1} \text{ yr}^{-1}$) and third decade ($EF_{\text{modeled } CO_2 \text{ onsite } 10-30 \text{ year}} = 1.8 \pm 0.3 \text{ Mg C ha}^{-1} \text{ yr}^{-1}$) (Fig. 6a).

Mean annual and decadal modeled N_2O emissions stemming from peat decomposition ($EF_{\text{modeled } N_2O \text{ decomp}}$) are compared with the IPCC default, and in situ values, in Fig. 7a. Modeled annual N_2O emissions from peat decomposition were highly variable over time with a large standard error

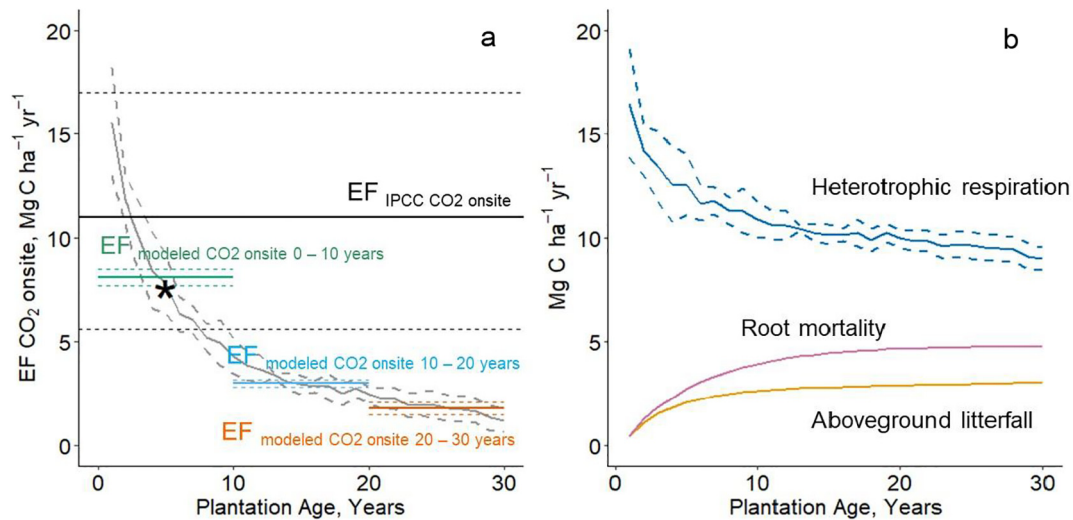


Fig. 6. Peat onsite CO_2 emissions ($\text{EF}_{\text{CO}_2 \text{ onsite}}$, equal to the difference between C inputs to peat from aboveground litterfall and root mortality and C outputs from heterotrophic respiration) (a) and components (b). Panel (a) presents annual average peat onsite CO_2 emissions predicted by DNDC (grey line, $n = 3$) and decadal averages (0–10 years green line, 10–20 years light blue line, 20–30 years red line, $n = 10$). Dashed lines are standard errors. The star indicates mean peat onsite CO_2 emissions determined from in situ observations and literature values (Swails et al., 2021). The IPCC default peat onsite CO_2 emission factor for oil palm plantations (Drösler et al., 2014) is indicated by the solid black line with its 95% confidence interval (dashed black lines). Panel (b) shows modeled heterotrophic respiration (dark blue line), root mortality (pink line), and aboveground litterfall (gold line) with dashed lines indicating standard error ($n = 3$). The standard errors of modeled litterfall and root mortality are not displayed given their low values (<5% of mean in year 1 and <1% of mean in following years).

reflecting the variation across the three plantations. The EF over the first decade ($\text{EF}_{\text{modeled N}_2\text{O decomp } 0-10 \text{ years}} = 3.5 \pm 0.3 \text{ kg N}_2\text{O ha}^{-1} \text{ yr}^{-1}$) increased over the following decades ($\text{EF}_{\text{modeled N}_2\text{O decomp } 10-20 \text{ years}} = 4.7 \pm 0.5 \text{ kg N}_2\text{O ha}^{-1} \text{ yr}^{-1}$ and $\text{EF}_{\text{modeled N}_2\text{O decomp } 20-30 \text{ years}} = 4.6 \pm 0.5 \text{ kg N}_2\text{O ha}^{-1} \text{ yr}^{-1}$). In all cases, the modeled EF was higher than the IPCC default ($\text{EF}_{\text{IPCC N}_2\text{O decomp}} = 1.2 \text{ kg N}_2\text{O ha}^{-1} \text{ yr}^{-1}$, Drösler et al., 2014).

Mean annual modeled N_2O emissions induced by N fertilizer application ($\text{EF}_{\text{modeled N}_2\text{O fert}}$) were substantially lower than rates obtained applying the IPCC EF (1.6% of N inputs) (Fig. 7b) and also substantially lower than

emissions from peat decomposition (Fig. 7a). $\text{EF}_{\text{modeled N}_2\text{O fert}}$ was on average 0.6% of N inputs over the 30-year rotation. Similar to N_2O emissions from peat decomposition, fertilizer-induced N_2O emissions were lower in the first decade ($\text{EF}_{\text{modeled N}_2\text{O fert } 0-10 \text{ years}} = 0.32 \pm 0.11\%$ of N inputs) than in the second decade and third decades of the rotation ($\text{EF}_{\text{modeled N}_2\text{O fert } 10-20 \text{ years}} = 0.73 \pm 0.24\%$ and $\text{EF}_{\text{modeled N}_2\text{O fert } 20-30 \text{ years}} = 0.84 \pm 0.27\%$). Both nitrification and denitrification in the topsoil (0–10 cm) layer contributed to fertilizer-induced N_2O emissions, while N_2O emissions from peat decomposition were exclusively generated through nitrification (Fig. S5).

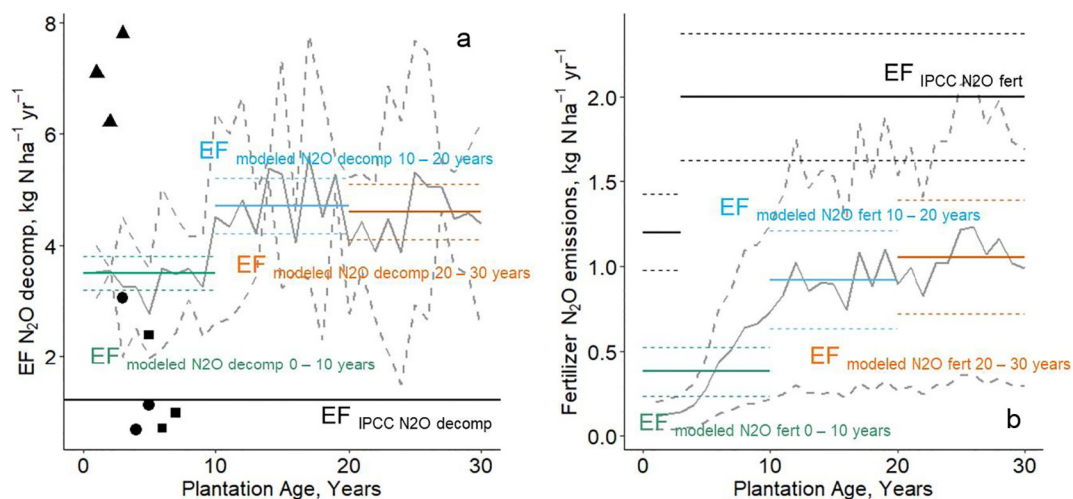


Fig. 7. Peat N_2O emissions stemming from peat decomposition ($\text{EF}_{\text{N}_2\text{O decomp}}$) (a) and fertilizer-induced N_2O emissions (b). Note different y-axis scales in (a) and (b). Modeled emissions over the 30-year rotation period are represented by a solid grey line in (a) and (b) with dashed grey lines indicating standard error ($n = 3$). Panels (a) and (b) present average annual modeled emissions during the first (green line), second (light blue line) and third (red line) decade with dashed lines indicating standard errors ($n = 10$). In situ measurement of mean annual peat decomposition N_2O emissions in our plots (Sep 2012 – Aug 2013, Sep 2013 – Aug 2014, Sep 2014 – Sep 2015) are represented by triangles (OP-2011), circles (OP-2009), and squares (OP-2007) in (a). The black line in (a) presents the IPCC default EF for emissions from peat decomposition in oil palm plantations ($1.2 \text{ kg N ha}^{-1} \text{ yr}^{-1}$, no error as the estimate was based on a single value). In (b) the black line indicates N fertilizer-induced emissions computed from the IPCC default EF (1.6% of N inputs) with dashed lines indicating the upper and lower bounds of the 95% CI. Plantations were simulated to receive $75 \text{ kg N ha}^{-1} \text{ yr}^{-1}$ for the first three years and $125 \text{ kg N ha}^{-1} \text{ yr}^{-1}$ thereafter following common practice in Southeast Asia (Darmosarkoro et al., 2003).

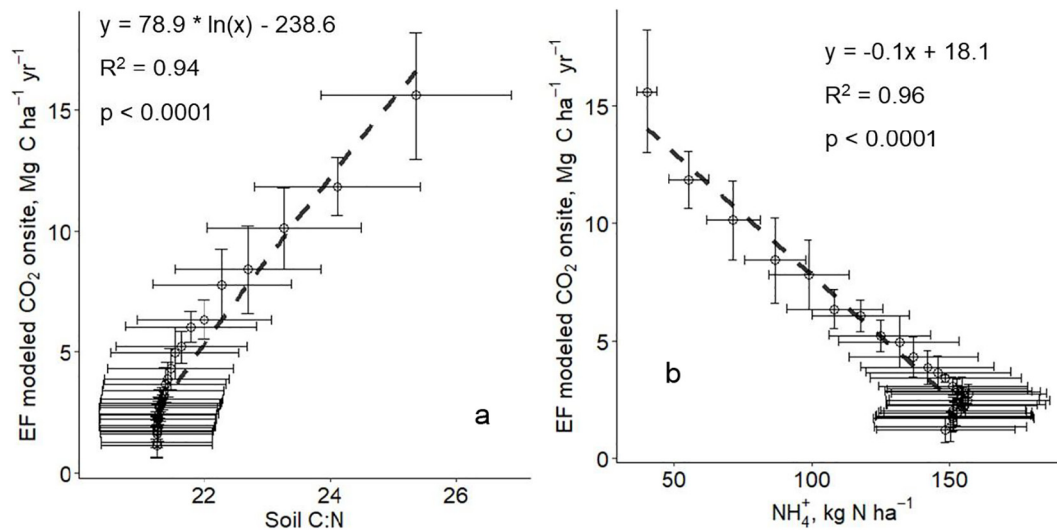


Fig. 8. Mean annual modeled peat onsite CO₂ emissions ($EF_{\text{modeled CO}_2 \text{ onsite}}$) as a function (dashed grey line) of modeled soil C:N ratio (a) and soil NH₄⁺ content in the topsoil layer (0–10 cm) (b). Each data point represents the average of the three plots in each year of the 30-year simulation and the vertical and horizontal bar are its associated standard error ($n = 30$).

Additional model outputs related to peat N₂O emissions – rates of N mineralization, nitrification and denitrification as well as soil NH₄⁺ and NO₃⁻ content (Fig. S5), N uptake by oil palm (Fig. S6), and peat NH₃ fluxes and rates of NO₃⁻ leaching (Fig. S7) – are presented in the Supplementary Information (S6).

3.3.2. Relationships between peat EF and environmental factors

Modeled annual peat onsite CO₂ emissions ($EF_{\text{modeled CO}_2 \text{ onsite}}$) increased logarithmically with increasing soil C:N ratio (Fig. 8a) and decreased linearly with increasing soil NH₄⁺ content in the topsoil layer (0–10 cm) (Fig. 8b). $EF_{\text{modeled CO}_2 \text{ onsite}}$ was not related to annual precipitation, water table level, soil WFPS, or soil NO₃⁻ content.

Modeled annual N₂O emissions stemming from peat decomposition ($EF_{\text{modeled N}_2\text{O decomp}}$) increased linearly with increasing total annual precipitation and rising water table level (Fig. 9a, b respectively), and increased exponentially with growing topsoil (0–10 cm) NH₄⁺ content (Fig. 9c). Multiple linear regression with precipitation and topsoil NH₄⁺ content explained 86% of variation in peat decomposition N₂O emissions ($p < 0.0001$). $EF_{\text{modeled N}_2\text{O decomp}}$ was not related to soil WFPS or NO₃⁻ content.

$EF_{\text{modeled N}_2\text{O fert}}$ decreased exponentially with increasing soil C:N ratio (Fig. 10a) and increased exponentially with increasing soil mineral N content (NO₃⁻ + NH₄⁺) in the topsoil layer (Fig. 10b). Fertilizer-induced N₂O emissions were also related to total annual precipitation and water table level, but the models poorly explained variation in $EF_{\text{modeled N}_2\text{O fert}}$ ($R^2 < 0.25$).

4. Discussion

4.1. Model application and limitations

To account for the variability of vegetation and management in oil palm plantations and associated soil and plant processes, we ran the DNDC model for two spatial positions (close to palm and far from palm) where soil GHG fluxes and environmental variables were collected in situ. This approach has been previously applied for representation of micro-spatial variation in plot-scale simulations of agro-ecosystems using DNDC (e.g., Deng et al., 2018) and other process-based models (e.g., Hergoualch et al., 2009). While it allows simulating fertilizer application around palms and disaggregating N₂O emissions per N source (SOM versus N input), the approach also presents several limitations. For instance, the two spatial positions are independent from each other in the simulations thereby their interactions, like C and N lateral transfers, are not considered in our analysis. Furthermore,

all C inputs were simulated to occur in the CT area (since the FT position was bare soil) and aboveground litterfall was simulated to be even over time while in practice, fronds are cut monthly during fruit harvest and piled in stacks between palms. However, the impact on peat onsite CO₂ and N₂O emissions of simulating an even distribution of aboveground litterfall C inputs in space and time may be minimal according to findings by Manning et al. (2019). While the spatial distribution of belowground carbon inputs from root mortality have not been well characterized in oil palm plantations, root density is usually highest in the 2-m radius around palms. However, roots can extend up to 5 m from the palm base (Khalid et al., 1999), where the FT position was located. According to Nelson et al. (2006) and Goodrick et al. (2016) roots are potentially less active further from palms in taking up nutrients and contributing to OM incorporation to the soil. Nevertheless, to test bias associated with our approach field measurements are needed to better characterize the spatially heterogeneous influence of root processes such as OM input from mortality on heterotrophic respiration and peat decomposition N₂O emissions.

With regards to model performance, DNDC simulated well the magnitude and fluctuations of key controls of soil GHG fluxes like the water table level and soil WFPS (Fig. 3). However, the model overestimated soil temperature in the oldest plantation (Fig. 3), where the effect of canopy shading at the CT position was not adequately captured. This bias seemed to have a minimal impact on the results of this study given that soil temperature was not a key variable explaining variation in the simulated emission factors (Figs. 8–10). Observations of the influence of soil temperature on heterotrophic respiration and N₂O emissions stemming from peat decomposition in oil palm plantations are inconsistent, with some studies detecting a positive relationship between soil temperature and peat GHG fluxes (Chaddy et al., 2019; Manning et al., 2019; Oktarita et al., 2017) and other studies detecting no influence (Comeau et al., 2013; Marwanto and Agus, 2014) similarly as at our research sites (Swails et al., 2018; Swails et al., 2021). Different trends among research studies may be due to a disparity in the amplitude of temperature variation during the experimental period, a difference in the level of shade depending on the age of palms as well as a dissimilarity in temperature sensitivity related to SOM quality (Davidson and Janssens, 2006). Even so, the magnitude of in situ GHG emission variation associated with temperature changes may remain limited in the humid tropics where diurnal, seasonal, and inter-annual fluctuations are small (Comeau et al., 2016; Kiew et al., 2020; Oktarita et al., 2017).

Average modeled C inputs to the peat from aboveground litterfall and root mortality over the 30-year rotation were within the ranges of rates

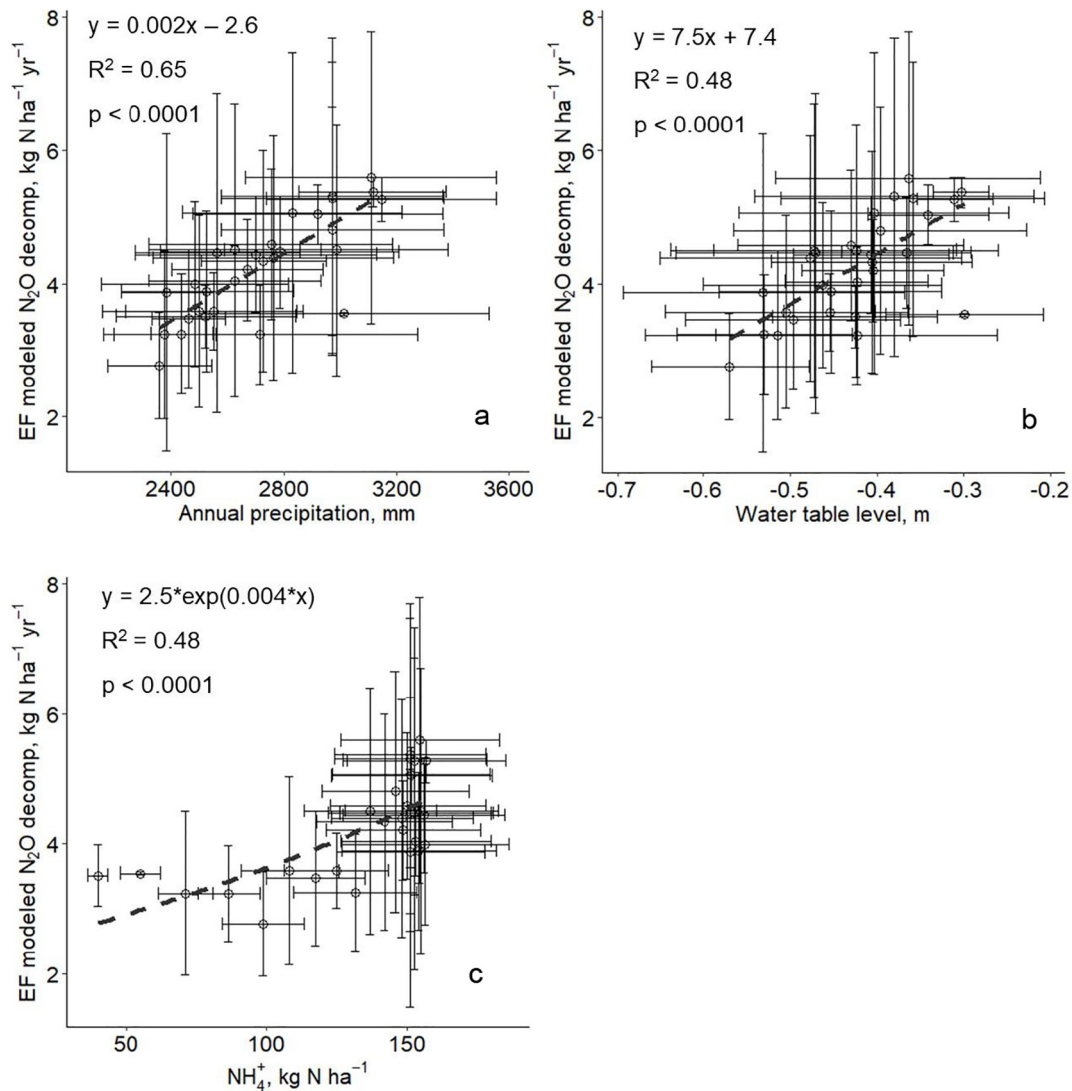


Fig. 9. Mean annual modeled N_2O emissions from peat decomposition ($\text{EF}_{\text{modeled N}_2\text{O decomp}}$) as a function (dashed grey line) of annual precipitation (a) and modeled mean annual water table level (b) and soil NH_4^+ content in the topsoil layer (0–10 cm) (c). Each data point represents the average of the three plots in each year of the 30-year simulation and the vertical and horizontal bar are its associated standard error ($n = 30$). Water table levels below the soil surface are indicated by negative values.

reported in the literature (Fig. 2c, d). However, published measurements of root mortality in oil palm plantations are highly variable and differ widely depending on local conditions (Henson and Chai, 1997; Lamade and Bouillet, 2005). Modeled C outputs from heterotrophic respiration were close to in situ observations (Fig. 5b) and were sensitive to the initial size of the litter pool fraction of SOM (Table S3). The main shortcoming of DNDC was its inability to simulate the full magnitude of fluctuation among observations in mean annual N_2O emissions from peat decomposition (Fig. 5c). The model captured the higher emissions in OP-2011 than in the other plantations (Fig. 5c) owing to the sensitivity of simulated peat decomposition N_2O emissions to the initial size of the SOM humad pool and corresponding initial humad fractions at the sites (Table S3). However, DNDC overestimated annual emissions in OP-2007 and OP-2009, and underestimated emissions in OP-2011, potentially as a result of a failure to simulate, respectively, N_2O uptake in the oldest and intermediate-age plantations and pulses of N_2O in the youngest plantation. Indeed, in OP-2007 and OP-2009, in situ N_2O uptake by peat represented close to 10% of the mean net annual N_2O flux (Swails et al., 2021). N_2O consumption is not uncommon across the tropics (Chapuis-Lardy et al., 2007) and has been observed in Southeast Asian and South American peatlands (e.g. Hergoualc'h et al., 2020; Jauhainen et al., 2011; Takakai et al., 2006). It is usually promoted by low nitrate availability, high WFPS and more generally by

conditions inhibiting N_2O diffusion in the soil (Chapuis-Lardy et al., 2007) as observed at the sites (Fig. 3, Table S2). In order to simulate N_2O uptake by peat, the model needs to incorporate relevant processes consuming N_2O in soils and simulate impacts of environmental factors on these processes. In OP-2011, in situ pulses of N_2O flux which occurred far from palms in half of the chambers had a large influence on annual N_2O emissions (Swails et al., 2021). While site-specific drivers of these pulses are unclear, hot spots of N_2O emissions from peat in oil palm plantations have previously been linked to high rates of net mineralization measured in vitro suggesting that microbial or fungal community composition could play a role (Oktarita et al., 2017). The combination of biogeophysical drivers stimulating transient, sporadic, or longer-term conditions driving extremely large pulses of N_2O emissions from peat decomposition requires further investigation in order to appropriately simulate hot spots of N_2O flux using process-based models.

4.2. Peat onsite CO_2 EF

The onsite CO_2 EF is critical to GHG inventories in oil palm plantations, given that in drained peatlands over 90% of peat GHG emissions are released as CO_2 (Swails et al., 2021). DNDC offered the possibility to simulate all C fluxes that contribute to the peat onsite CO_2 EF (heterotrophic

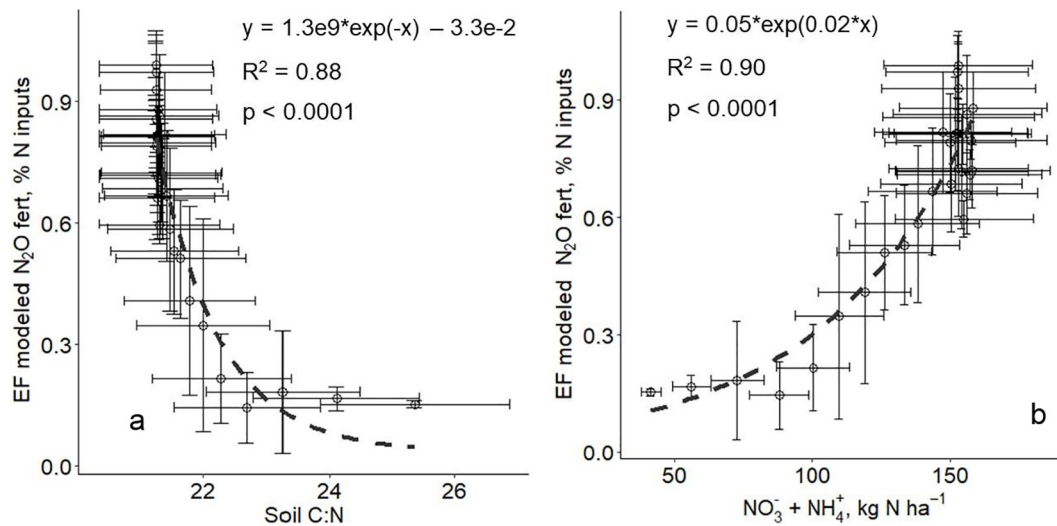


Fig. 10. Mean annual modeled fertilizer-induced N_2O emissions expressed as a percentage of N inputs ($\text{EF}_{\text{modeled N}_2\text{O fert}}$) as a function (dashed grey line) of modeled soil C:N ratio (a) and total mineral N content ($\text{NO}_3^- + \text{NH}_4^+$) in the topsoil layer (0–10 cm) (b). Each data point represents the average of the three plots in each year of the 30-year simulation and the vertical and horizontal bar are its associated standard error ($n = 30$).

respiration, litterfall, root mortality) and to investigate temporal change of these fluxes and their balance. Simulation of the full 30-year oil palm rotation indicated that the $\text{EF}_{\text{modeled CO}_2 \text{ onsite}}$ declined over time as the result of a larger decrease in heterotrophic respiration rate than the corresponding increase in C inputs (Fig. 6b). The model predicted that the initial large decomposition rates were not sustained, and this decrease was highly positively correlated to reduced fraction of the litter pool, the most labile pool contributing to SOM (Fig. S4b). This result is in agreement with observations from ex situ experiments indicating that land-use change renders tropical peat more recalcitrant to decomposition (Jauhiainen et al., 2016; Könönen et al., 2016), implying that soil heterotrophic respiration from a drained tropical peatland will decline over time (Swails et al., 2018). Mechanistically, the reduction in C decomposition rate can be explained by preferential consumption by microbes of labile C compounds, leading to increased ratio of recalcitrant to labile C compounds in degraded peat soils (Könönen et al., 2016; Swails et al., 2018; Wright et al., 2011). While chrono-sequential in situ experiments on soil heterotrophic respiration remain limited to young oil palm plantations (Hergoualc'h et al., 2017), Cooper et al. (2020) observed a 50% decrease in a mature plantation as compared to a young plantation in soil respiration measured 3.5 m away from palm trunks and assumed as representative of heterotrophic respiration by these authors. Similarly, a long-term whole ecosystem monitoring study by McCalmont et al. (2021) found a 51% reduction in peat carbon losses in the first 6 years as compared to the following 7 years of an oil palm plantation chronosequence. The decrease of the modeled $\text{EF}_{\text{CO}_2 \text{ onsite}}$ over time suggests that the $\text{EF}_{\text{IPCC CO}_2 \text{ onsite}}$ ($11 \text{ Mg C ha}^{-1} \text{ yr}^{-1}$) which was developed based on young plantations could be refined by reducing its value by 61% and 77%, respectively, for the second decade ($4.3 \text{ Mg C ha}^{-1} \text{ yr}^{-1}$) and third decade ($2.5 \text{ Mg C ha}^{-1} \text{ yr}^{-1}$) after planting, or by 69% on average for the last two decades ($3.4 \text{ Mg C ha}^{-1} \text{ yr}^{-1}$). Together with data on plantation age, either site-specific or derived from remote sensing approaches (e.g. Hansen et al., 2013), these refined EF could improve the accuracy of GHG accounting in these ecosystems.

The temporal decrease of the $\text{EF}_{\text{modeled CO}_2 \text{ onsite}}$ was associated with a decline in soil C:N ratio (Fig. 8a). Microbial transformation of organic matter depletes C more quickly than N, leading to declining soil C:N ratio with increasing peatland degradation (Leifeld et al., 2019). Moreover, the increased litter and root N inputs to the soil over time potentially contributed as well to a gradual decrease in the soil C:N ratio. The negative relationship between the $\text{EF}_{\text{modeled CO}_2 \text{ onsite}}$ and soil NH_4^+ content (Fig. 8b) corroborates the tight link between peat decomposition and N mineralization processes

both of which are affected by the quality of the organic matter, in particular the soil C:N ratio (Bayley et al., 2005). Many studies have observed that drainage of peatlands results in increased rates of N mineralization and nitrification and decreased rates of denitrification, leading to higher levels of soil mineral N (Groffman et al., 1984; Holden et al., 2004). In our simulation soil mineral N content – chiefly dominated by NH_4^+ – increased over time (Fig. S5a) as a result of net N mineralization rates that were higher than rates of nitrification (Fig. S5d). While these relationships should be further investigated across peatlands portraying a range of SOM quality and validated based on in situ data from plantations spanning the 30-year rotation, they are promising for predicting peat onsite CO_2 losses in oil palm plantations on peat.

Although water table level has been thoroughly investigated as a proxy for heterotrophic respiration from tropical peat soils (e.g. Carlson et al., 2015; Prananto et al., 2020), peat onsite CO_2 emissions are equal to the difference between C inputs from vegetation litter and C outputs from heterotrophic respiration. Furthermore, peat CO_2 loss rates in tropical peatlands vary greatly depending on pre-conversion land-use history and post-conversion plantation age and management practices (Hergoualc'h and Verchot, 2014; Hergoualc'h et al., 2017). Neither the modeled peat onsite CO_2 EF nor its individual components (heterotrophic respiration, litterfall, root mortality) were related to mean annual water table. The significant relationships among modeled peat onsite CO_2 EF, C:N ratio and peat NH_4^+ content suggests that peat chemistry exerted a stronger control on peat onsite CO_2 emissions than mean annual water table level over the 30-year rotation in the simulated oil palm plantations.

The $\text{EF}_{\text{modeled CO}_2 \text{ onsite}}$ in the first decade after plantation establishment generated by DNDC ($7.7 \pm 0.4 \text{ Mg C ha}^{-1} \text{ yr}^{-1}$) was lower but within the 95% confidence interval of the IPCC default ($11 \pm 5.5 \text{ Mg C ha}^{-1} \text{ yr}^{-1}$). The latter is based on flux measurements in relatively young plantations (median age of plantations = 7 years) and considers peat subsidence studies which may inflate estimates (Cooper et al., 2020; Kasimir-Klemetsson et al., 1997), especially in years following peat swamp forest conversion when the peat dome collapses and subsidence originates mainly from compaction and shrinking physical processes rather than chemical decomposition processes (Kool et al., 2006).

4.3. Peat decomposition N_2O EF

DNDC predicted increasing N_2O emissions from peat decomposition over the 30-year rotation with a notable difference between the first decade

and the latter decades ($+1.2 \text{ kg N ha}^{-1} \text{ yr}^{-1}$); a trend which followed the pattern of increased soil NH_4^+ content over time (Fig. S5b). The increase in $\text{EF}_{\text{modeled N}_2\text{O decomp}}$ suggests that the IPCC EF ($1.2 \text{ kg N ha}^{-1} \text{ yr}^{-1}$) could be increased by 34% in the latter two decades of a 30-year rotation to account for increased N_2O emissions with increasing availability of NH_4^+ . Nevertheless, it is important to note that the predicted rise in N_2O emissions over time does not offset the corresponding decrease in CO_2 emissions ($54 \text{ Mg CO}_{2\text{eq.}} \text{ ha}^{-1}$ over 30 years for N_2O versus $458 \text{ CO}_2 \text{ ha}^{-1}$ over 30 years for CO_2), indicating that total GHG emissions decline over the rotation.

Inter-annual variation in mean annual N_2O emissions from peat decomposition was robustly ($R^2 = 0.65$) related to annual precipitation. Positive feedback between soil N_2O emissions and precipitation was found to be relevant globally across biomes according to a meta-analysis of manipulative experiments (Yan et al., 2018). Since precipitation is easy to monitor it could serve as a useful proxy for monitoring N_2O emissions from oil palm plantations on peat. Modeled peat N_2O emissions also increased with increasing average annual water table level, but with a lower robustness than the relationship with precipitation ($R^2 = 0.48$). These relationships were not independent from each other since the average annual WT was positively and strongly correlated to annual precipitation ($R^2 = 0.79$). Peat decomposition N_2O emissions were found to be essentially a product of nitrification (Fig. S5b), therefore the positive relationship with soil NH_4^+ content stands to reason. Together, precipitation and soil NH_4^+ content explained 86% of variation in peat decomposition N_2O emissions, confirming the importance of dual moisture and substrate controls on N_2O emissions from SOM decomposition (Firestone and Davidson, 1989; Butterbach-Bahl et al., 2013).

The $\text{EF}_{\text{modeled N}_2\text{O decomp}}$ was three to four times higher than the IPCC EF ($1.2 \text{ kg N ha}^{-1} \text{ yr}^{-1}$). Assessments of annual N_2O emissions from peat decomposition in unfertilized oil palm plantations in the first decade of rotation (2–9 years) (Chaddy et al., 2019; Oktarita et al., 2017; Sakata et al., 2015) indicated even higher rates ($22.8 \pm 5.7 \text{ kg N ha}^{-1} \text{ yr}^{-1}$, $n = 8$) than our modeled results. The IPCC EF is based on flux measurements at a single site, while observations of annual N_2O emissions from peat decomposition vary greatly according to site and are known to be large in drained peatlands (Leifeld and Menichetti, 2018; Pärn et al., 2018; Tan et al., 2019). Additional field measurements of N_2O fluxes, particularly in oil palm plantations in the second and third decades of rotation, are crucially needed to reduce the uncertainty of peat decomposition N_2O fluxes.

4.4. Fertilizer-induced N_2O EF

Disentanglement of N_2O emissions stemming from peat decomposition and N fertilizer-induced N_2O emissions is difficult, and only feasible over short-term experiments with the application of ^{15}N -labeled fertilizer (Mosier and Klemetsson, 1994). Process-based models provide the opportunity to simulate unfertilized and fertilized scenarios while controlling other environmental variables, thereby supporting disaggregation of N_2O emissions by source. Fertilizer-induced N_2O emissions in oil palm plantations and in drained cultivated peatlands of the tropics in general have been poorly characterized (Pardon et al., 2016). These emissions, like N_2O emissions from peat decomposition, were higher in the second and third decades of the rotation ($0.73 \pm 0.24\%$ and $0.84 \pm 0.27\%$ of N inputs) compared to the first decade ($0.32 \pm 0.27\%$ of N inputs). Consistent with assessments indicating that oil palm N uptake stabilizes after the first years of growth, modeled N uptake by palms was steady in the second and third decades of the rotation (Fig. S6). This suggests a potential for increased N availability associated with N-fertilizer application exceeding vegetation demand to exacerbate N-fertilizer emissions. Fertilizer-induced N_2O emissions have been shown to increase exponentially with increasingly large mineral N surplus in agricultural soils (Shcherbak et al., 2014; van Groenigen et al., 2010).

The fertilized-induced emission factor increased with decreasing soil C:N ratio (Fig. 10a) and increasing mineral N content (Fig. 10b). A negative relationship between the emission factor and the soil C:N ratio among other variables was observed as a general tendency of agricultural soils in Canada (Rochette et al., 2018). The relationship is consistent with

increased nitrification rates resulting from fertilizer application (Fig. S5f) contributing to reduce the soil C:N ratio. While peat decomposition N_2O emissions increased as soil NH_4^+ contents rose, the fertilizer-induced emission factor was related to total soil mineral content. Urea application favored nitrification (Fig. S5f) thus providing increase in available soil NO_3^- content (Fig. S5c). Enhanced concentrations of soil mineral N (NH_4^+ and NO_3^-) as a result of long-term fertilization is pursuant to findings by Lu et al. (2011) based on empirical studies.

Modeled N-fertilizer emissions contributed only 16% to total N_2O emissions (from peat decomposition and N-fertilizer inputs) over the rotation, in agreement with observations from cultivated peatlands in Indonesia fertilized similarly to our site (Oktarita et al., 2017; Toma et al., 2011). The fertilized-induced N_2O emission factor (0.6% of N inputs over the 30-year rotation) was less than half of the IPCC EF ($\text{EF}_{\text{IPCC N}_2\text{O fert}}$) (1.6% of N inputs). It was also much lower than the country-specific emission factor for the Netherlands for fertilizer application on peat (3% of N inputs; Velthof and Rietra, 2018). In wet climates high soil C content and low soil pH typically favor a high EF (Hergoualc'h et al., 2021) but urea as the form of the fertilizer (Hergoualc'h et al., 2019) and high temperatures, common in opened tropical peatlands, promote high gaseous NH_3 losses (Ernst and Massey, 1960; He et al., 1999). DNDC predicted high volatilization losses (16% of N inputs) as well as significant N losses via leaching (2%). Together these important pathways of N loss (Fig. S7) may partly explain low N_2O emissions from N-fertilizer at our sites.

5. Conclusions

DNDC's simulated peat GHG fluxes (CO_2 and N_2O) and biogeophysical drivers (climate, soil, vegetation, and management practices) in oil palm plantations on peat allowed the generation of EF disaggregated by plantation age and emission source (decomposition, fertilizer-induced), a practical and useful application for GHG inventories in tropical peatlands. Model predictions suggested that IPCC default EF for oil palm, based on limited observations in predominantly young plantations, may overestimate peat onsite CO_2 emissions and underestimate N_2O emissions from peat decomposition in the later decades of the rotation. They also resulted in peat N_2O emissions stemming from synthetic N fertilizer inputs lower than the IPCC default EF. Our study highlights the importance of biogeochemical controls on oil palm peat EF in addition to physical controls. Soil C:N ratio and mineral N content, in addition to precipitation, and water table level, were identified as suitable proxies for refining peat EF for oil palm plantations. Our analysis also highlighted the need for additional field studies to increase understanding of and better represent soil processes in tropical peatlands and their influence on peat GHG emissions, particularly the magnitude and spatial distribution of C inputs to peat from aboveground litterfall and root mortality, the biogeophysical conditions driving hot spots and hot moments of peat N_2O flux, and the influence of changes in SOM quality over time on heterotrophic respiration and N_2O emissions from peat decomposition and N-fertilizer inputs. Additional empirical studies in older plantations are crucially needed to validate model predictions and refine oil palm peat GHG EF.

CRedit authorship contribution statement

Erin Swails: Conceptualization, Investigation, Formal analysis, Writing – Original draft preparation **Kristell Hergoualc'h:** Conceptualization, Resources, Formal analysis, Writing – Review & Editing **Jia Deng:** Conceptualization, Software, Writing – Review & Editing **Steve Frolking:** Conceptualization, Writing – Review & Editing **Nisa Novita:** Investigation, Writing – Review & Editing.

Funding

This research was conducted under the Sustainable Wetlands Adaptation and Mitigation Program (SWAMP) and was generously supported by

the governments of the United States of America (Grant MTO-069033) and Norway (QZA-21/-124). It was undertaken as part of the CGIAR research program on Climate Change, Agriculture and Food Security (CCAFS).

Declaration of competing interest

The authors declare that they have no known competing financial interests or personal relationships that could have appeared to influence the work reported in this paper.

Acknowledgements

The authors are grateful to the staff of Tanjung Puting National Park for facilitating the study and providing lodging. We would also like to thank all assistants and villagers for their continuous help in the field, and also Desti Hertanti for her indispensable support to collect data, and Novi Wahyuni for her critical work in analyzing GHG concentrations. The constructive comments by the anonymous reviewers greatly improved the manuscript and are much appreciated.

Appendix A. Supplementary data

Supplementary data to this article can be found online at <https://doi.org/10.1016/j.scitotenv.2022.156153>.

References

Bayley, S.E., Thormann, M.N., Szumigalski, A.R., 2005. Nitrogen mineralization and decomposition in western boreal bog and fen peat. *Ecoscience* 12, 455–465.

Butterbach-Bahl, K., Baggs, E.M., Dannemann, M., Kiese, R., Zechmeister-Boltenstern, S., 2013. Nitrous oxide emissions from soils: how well do we understand the processes and their controls? *Philos. Trans. R. Soc.*, B 368, 20130122.

Carlson, K.M., Goodman, L.K., May-Tobin, C.C., 2015. Modeling relationships between water table depth and peat soil carbon loss in Southeast Asian plantations. *Environ. Res. Lett.* 10, 074006.

Chaddy, A., Melling, L., Ishikura, K., Hatano, R., 2019. Soil N₂O emissions under different N rates in an oil palm plantation on tropical peatland. *Agriculture* 9, 213.

Chapuis-Lardy, L., Wrage, N., Metay, A., Chotte, J.L., Bernoux, M., 2007. Soils, a sink for N₂O? A review. *Glob. Chang. Biol.* 13, 1–17.

Comeau, L.P., Hergoualc'h, K., Smith, J., Verchot, L.V., 2013. Conversion of Intact Peat Swamp Forest to Oil Palm Plantation: Effect on Soil CO₂ Fluxes in Jambi, Sumatra. Working Paper 110. CIFOR, Bogor, Indonesia.

Comeau, L.P., Hergoualc'h, K., Hartill, J., Smith, J.U., Verchot, L.V., Peak, D., Salim, A.M., 2016. How do the heterotrophic and the total soil respiration of an oil palm plantation on peat respond to nitrogen fertilizer application? *Geoderma* 268, 41–51.

Cooper, H.V., Evers, S., Aplin, P., Crout, N., Dahalan, M.P.B., Sjögersten, S., 2020. Greenhouse gas emission resulting from conversion of peat swamp forest to oil palm plantation. *Nat. Commun.* 11, 407.

Darmasarkoro, W., Sutarta, E.S., Winarna, 2003. Teknologi pemupukan tanaman kelapa sawit dalam lahan dan pemupukan Kelapa Sawit (Medan: Pusat Penelitian Kelapa Sawit), pp. 113–134.

Davidson, E.A., Janssens, I.A., 2006. Temperature sensitivity of soil carbon decomposition and feedbacks to climate change. *Nature* 440, 165–173.

Deng, J., Li, C., Frolking, S., Zhang, Y., Bäckstrand, K., Crill, P., 2014. Assessing effects of permafrost thaw on C fluxes based on multiyear modeling across a permafrost thaw gradient at Stordalen, Sweden. *Biogeosciences* 11, 4753–4770.

Deng, J., McCalley, C.K., Frolking, S., Chanton, J., Crill, P., Varner, R., et al., 2017. Adding stable carbon isotopes improves model representation of the role of microbial communities in peatland methane cycling. *J. Adv. Model. Earth Syst.* 9, 1412–1430.

Deng, J., Li, C., Burger, M., Horwath, W.R., Smart, D., Six, J., et al., 2018. Assessing short-term impacts of management practices on N₂O emissions from diverse Mediterranean agricultural ecosystems using a biogeochemical model. *J. Geophys. Res. Biogeosci.* 123, 1557–1571.

Dresscher, J., Rembold, K., Allen, K., Beckschäfer, P., Buchori, D., Clough, Y., et al., 2016. Ecological and socio-economic functions across tropical land use systems after rainforest conversion. *Philos. Trans. R. Soc.*, B 371, 20150275.

Dröslér, M., Verchot, L.V., Freibauer, A., Pan, G., Evans, C.D., Bourbonniere, R.A., et al., 2014. Chapter 2: drained inland organic soils. In: Hiraishi, T., Krug, T., Tanabe, K., Srivastava, N., Jamsranjav, B., Fukuda, M., et al. (Eds.), Supplement to the 2006 Guidelines for National Greenhouse Gas Inventories: Wetlands. Intergovernmental Panel on Climate Change, Switzerland.

Ernst, J.W., Massey, H.F., 1960. The effects of several factors on volatilization of ammonia formed from urea in the soil. *Soil Sci. Soc. Am. J.* 24, 87–90.

Farmer, J., Matthews, R., Smith, J.U., Smith, P., Singh, B.K., 2011. Assessing existing peatland models for their applicability for modelling greenhouse gas emissions from tropical peat soils. *Curr. Opin. Environ. Sustain.* 3, 339–349.

Firestone, M.K., Davidson, E.A., 1989. Microbiological basis of NO and N₂O production and consumption in soil. In: Andreae, M.O., Schimel, D.S. (Eds.), Exchange of Trace Gases Between Terrestrial Ecosystems and the Atmosphere. John Wiley & Sons Ltd., pp. 7–21.

Frolking, S., Roulet, N.T., Tuittila, E., Bubier, J.L., Quillet, A., Talbot, J., Richard, P.J.H., 2010. A new model of Holocene peatland net primary production, decomposition, water balance, and peat accumulation. *Earth Syst. Dyn.* 1, 1–21.

Frolking, S., Talbot, J., Jones, M.C., Treat, C.C., Kauffman, J.B., Tuittila, E.S., Roulet, N., 2011. Peatlands in the Earth's 21st century climate system. *Environ. Rev.* 19, 371–396.

Germer, J., Sauerborn, J., 2008. Estimation of the impact of oil palm plantation establishment on greenhouse gas balance. *Environ. Dev. Sustain.* 10, 697–716.

Gilhespy, S.L., Anthony, S., Cardenas, L., Chadwick, D., del Prado, A., Li, C., et al., 2014. First 20 years of DNDC (DeNitrification DeComposition): model evolution. *Ecol. Model.* 292, 51–62.

Giltrap, D.L., Li, C., Saggari, S., 2010. DNDC: a process-based model of greenhouse gas fluxes from agricultural soils. *Agric. Ecosyst. Environ.* 136, 292–300.

Goodrick, I., Nelson, P.N., Nake, S., Webb, M., Bird, M., Huth, N., 2016. Tree-scale spatial variability of soil carbon cycling in a mature oil palm plantation. *Soil Res.* 54, 397–406.

van Groenigen, J.W., Velthof, G.L., Oenema, O., van Groenigen, J.V., van Kessel, C., 2010. Towards an agronomic assessment of N₂O emissions: a case study for arable crops. *Eur. J. Soil Sci.* 61, 903–913.

Groffman, P.M., Box, J.E., Todd, R.L., 1984. Effects of artificial drainage on soil mineral nitrogen dynamics in winter wheat on the southern piedmont. *Commun. Soil Sci. Plant Anal.* 15, 1051–1063.

Gumbrecht, T., Roman-Cuesta, R.M., Verchot, L., Herold, M., Wittmann, F., Householder, E., et al., 2017. An expert system model for mapping tropical wetlands and peatlands reveals South America as the largest contributor. *Glob. Chang. Biol.* 23, 3581–3599.

Hansen, M.C., Potapov, P.V., Moore, R., Hancher, M., Turubanova, S.A., Tyukavina, A., et al., 2013. High-resolution global maps of 21st-century forest cover change. *Science* 342, 850–853.

He, Z.L., Alva, A.K., Calvert, D.V., Banks, D.J., 1999. Ammonia volatilization from different fertilizer sources and effects of temperature and soil pH. *Soil Sci.* 164, 750–758.

Henson, I.E., Chai, S.H., 1997. Analysis of oil palm productivity: II. Biomass, distribution, productivity and turnover of the root system. *Elaeis* 9, 78–92.

Henson, I.E., Dolmat, M.T., 2003. Physiological analysis of an oil palm density trial on a peat soil. *J. Oil Palm Res.* 15, 1–27.

Hergoualc'h, K., Verchot, L., 2012. Changes in soil CH₄ fluxes from the conversion of tropical peat swamp forests: a meta-analysis. *J. Integr. Environ. Sci.* 9, 31–39.

Hergoualc'h, K., Verchot, L., 2014. Greenhouse gas emission factors for land use and land-use change in Southeast Asian peatlands. *Mitig. Adapt. Strateg. Glob. Chang.* 19, 789–907.

Hergoualc'h, K., Harmand, J.M., Cannavo, P., Skiba, U., Oliver, R., Hénault, C., 2009. The utility of process-based models for simulating N₂O emissions from soils: a case study based on Costa Rican coffee plantations. *Soil Biol. Biochem.* 41, 2343–2355.

Hergoualc'h, K., Hendry, D.T., Murdiyarso, D., Verchot, L., 2017. Total and heterotrophic soil respiration in a swamp forest and oil palm plantations on peat in Central Kalimantan, Indonesia. *Biogeochemistry* 135, 203–220.

Hergoualc'h, K., Akiyama, H., Bernoux, M., Chrinda, N., del Prado, A., Kasimir, A., et al., 2019. Chapter 11: N₂O emissions from managed soils and CO₂ emissions from lime and urea application. In: Calvo Buendia, E., Tanabe, K., Kranjc, A., Baasansuren, J., Fukuda, M., Ngarize, S., et al. (Eds.), 2019 Refinement to the 2006 Guidelines for National Greenhouse Gas Inventories – Volume 4 Agriculture, Forestry, and Other Land Use. Intergovernmental Panel on Climate Change, Switzerland.

Hergoualc'h, K., Dezzee, N., Verchot, L.V., Marius, C., van Lent, J., del Agua-Pasquel, J., et al., 2020. Spatial and temporal variability of soil N₂O and CH₄ fluxes along a degradation gradient in a palm swamp peat forest in the Peruvian Amazon. *Glob. Chang. Biol.* 26, 7198–7216.

Hergoualc'h, K., Mueller, N., Bernoux, M., Kasimer, A., van der Weerden, T.J., Ogle, S.M., 2021. Improved accuracy and reduced uncertainty in greenhouse gas inventories by refining the IPCC emission factor for direct N₂O emissions from nitrogen inputs to managed soils. *Glob. Chang. Biol.* 27, 6536–6550.

Holden, J., Chapman, P.J., Labadz, J., 2004. Artificial drainage of peatlands: hydrological and hydrochemical processes and wetland restoration. *Prog. Phys. Geogr.* 28, 95–123.

Huang, Y., Giais, P., Luo, Y., Zhu, D., Wang, Y., Qiu, C., et al., 2021. Tradeoff of CO₂ and CH₄ emissions from global peatlands under water-table drawdown. *Nat. Clim. Chang.* 11, 618–622.

Itoh, M., Okimoto, Y., Hirano, T., Kusin, K., 2017. Factors affecting oxidative peat decomposition due to land use in tropical peat swamp forests in Indonesia. *Sci. Total Environ.* 609, 906–915.

Jauhainen, J., Sivenoinen, H., Hamalainen, R., Kusin, K., Limin, S., Raison, R.J., Vasandar, H., 2011. Nitrous oxide fluxes from tropical peat with different disturbance history and management. *Biogeosciences* 9, 1337–1350.

Jauhainen, J., Sivenoinen, H., Könönen, M., Limin, S., Vasandar, H., 2016. Management driven changes in carbon mineralization dynamics of tropical peat. *Biogeochemistry* 129, 115–132.

Kasimir-Klemetsson, A., Klemetsson, L., Berglund, K., Martikainen, P., Silvola, J., Oenema, O., 1997. Greenhouse gas emissions from farmed organic soils: a review. *Soil Use Manag.* 13, 245–250.

Kettunen, A., 2003. Connecting methane fluxes to vegetation cover and water table fluctuations at microsite level: a modeling study. *Glob. Biogeochem. Cycles* 17, 1051.

Khalid, H., Zin, Z.Z., Anderson, J.M., 1999. Quantification of oil palm biomass and nutrient value in mature plantation: II. Below-ground biomass. *J. Oil Palm Res.* 11, 63–71.

Khasanah, N., van Noordwijk, M., Ningsih, H., 2015. Aboveground carbon stocks in oil palm plantations and the threshold for carbon-neutral vegetation conversion in mineral soils. *Cogent Environ. Sci.* 1, 1119964.

- Kiew, F., Hirata, R., Hirano, T., Xhuan, W.G., Aries, E.B., Kemudang, K., et al., 2020. Carbon dioxide balance of an oil palm plantation established on tropical peat. *Agric. For. Meteorol.* 295, 108189.
- Koboyashi, K., Salam, M.U., 2000. Comparing simulated and measured values using mean squared deviation and its components. *Agron. J.* 92, 345–352.
- Könönen, M., Jauhainen, J., Laiho, R., Spetz, P., Kusin, K., Limin, S., Vasandar, H., 2016. Land use increases the recalcitrance of tropical peat. *Wetl. Ecol. Manag.* 24, 717–731.
- Kool, D.M., Buurman, P., Hoekman, D.H., 2006. Oxidation and compaction of a collapsed peat dome in Central Kalimantan. *Geoderma* 137, 217–225.
- Kotowska, M.M., Leuschner, C., Triadiati, T., Hertel, D., 2016. Conversion of tropical lowland forest reduces nutrient return through litterfall, and alters nutrient use efficiency and seasonality of net primary production. *Oecologia* 180, 601–618.
- Kurnianto, S., Warren, M., Talbot, J., Kauffman, B., Murdiyarso, D., Frohling, S., 2015. Carbon accumulation of tropical peatlands over millennia: a modeling approach. *Glob. Chang. Biol.* 21, 431–444.
- Lamade, E., Bouillet, J.P., 2005. Carbon storage and global change: the role of oil palm. *Oléagineux, Corps Gras, Lipides* 12, 154–160.
- Lamade, E., Setiyo, I.E., 2002. Characterisation of carbon pools and dynamics for oil palm and forest ecosystems: application to environmental evaluation. *Enhancing Oil Palm Industry Development Through Environmentally Friendly Technology: Proceedings of Agriculture Conference, 2002 International Oil Palm Conference, Nusa Dua, Bali, July 8–12, 2002.*
- Lamade, E., Djégui, N., Leterme, P., 1996. Estimation of carbon allocation to the roots from soil respiration measurements of oil palm. *Plant Soil* 181, 329–339.
- Leifeld, J., Menichetti, L., 2018. The underappreciated potential of peatlands in global climate change mitigation strategies. *Nat. Commun.* 9, 1071.
- Leifeld, J., Wüst-Galley, C., Page, S., 2019. Intact and managed peatland soils as a source and sink of GHGs from 1850 to 2100. *Nat. Clim. Chang.* 9, 945–947.
- Li, C., 2000. Modeling trace gas emissions from agricultural ecosystems. In: Wassmann, R., Lanti, R.S., Neue, H.U. (Eds.), *Methane Emissions From Major Rice Ecosystems in Asia*. Springer, Netherlands, pp. 259–276.
- Li, C., Frohling, S., Frohling, T.A., 1992. A model of nitrous oxide evolution from soil driven by rainfall events: 1. Model structure and sensitivity. *J. Geophys. Res. Atmos.* 97, 9759–9776.
- Li, C., Frohling, S., Harriss, R., 1994a. Modeling carbon biogeochemistry in agricultural soils. *Glob. Biogeochem. Cycles* 8, 237–254.
- Li, C., Frohling, S., Harriss, R., Terry, R., 1994b. Modeling nitrous oxide emissions from agriculture: a Florida case study. *Chemosphere* 28, 1401–1415.
- Li, C., Aber, J., Stange, F., Butterbach-Bahl, K., Papen, H., 2000. A process-oriented model of N₂O and NO emissions from forest soils: 1. Model development. *J. Geophys. Res. Atmos.* 105, 4369–4384.
- Li, C., Trettin, C., Ge, S., McNulty, S., Butterbach-Bahl, K., 2005. Modelling carbon and nitrogen biogeochemistry in forest ecosystems. *3rd International Nitrogen Conference*, pp. 893–898.
- Li, C., Salas, W., Zhang, R., Krauter, C., Rotz, A., Mitloehner, F., 2012. Manure-DNDC: a biogeochemical process model for quantifying greenhouse gas and ammonia emissions from livestock manure systems. *Nutr. Cycl. Agroecosyst.* 93, 163–200.
- Lu, M., Yang, Y., Luo, Y., Fang, C., Zhou, X., Chen, J., et al., 2011. Response of ecosystem nitrogen cycle to nitrogen addition: a meta-analysis. *New Phytol.* 189, 1020–1050.
- Manning, F.C., Kho, L.K., Hill, T.C., Cornulier, T., Teh, Y.A., 2019. Carbon emissions from oil palm plantations on peat soil. *Front. For. Glob. Chang.* 2, 37.
- Marwanto, S., Agus, F., 2014. Is CO₂ flux from oil palm plantations on peatland controlled by soil moisture and/or soil and air temperatures? *Mitig. Adapt. Strateg. Glob. Chang.* 19, 809–819.
- McCalmont, J., Kho, L.K., Teh, Y.A., Lewis, K., Chocholek, M., Rumpang, E., Hill, T., 2021. Short- and long-term carbon emissions from oil palm plantations converted from logged tropical peat swamp forest. *Glob. Chang. Biol.* 27, 2361–2376.
- McGill, W.B., Hunt, H.W., Woodmansee, R.G., Reuss, J.O., 1981. Phoenix, a model of dynamics of carbon and nitrogen in grassland soils. *Ecol. Bull.* 33, 49–115.
- Melling, L., Hatano, R., Goh, K.J., 2005. Methane fluxes from three ecosystems in tropical peatlands of Sarawak, Malaysia. *Soil Biol. Biochem.* 37, 1445–1453.
- Mezbahuddin, M., Grant, R.F., Hirano, T., 2014. Modelling effects of seasonal variation in water table depth on net ecosystem CO₂ exchange of a tropical peatlands. *Biogeosciences* 11, 577–599.
- Miettinen, J., Hooijer, A., Shi, C., Tollenaar, D., Vermimmen, R., Liew, S.C., et al., 2012. Extent of industrial plantations on Southeast Asian peatlands in 2010 with analysis of historical expansion and future projections. *Glob. Chang. Biol. Bioenergy* 4, 908–918.
- Miettinen, J., Shi, C., Liew, S.C., 2016. Land cover distribution in the peatlands of Peninsular Malaysia, Sumatra and Borneo in 2015 with changes since 1990. *Glob. Ecol. Conserv.* 6, 67–78.
- Mosier, A.R., Klemetsson, L., 1994. Measuring denitrification in the field. In: Weaver, R.W., Angle, J.S., Bottomley, P.S. (Eds.), *Methods of Soil Analysis Part 2 Microbiological and Biochemical Properties*. Soil Science Society of America, Inc., pp. 1047–1065.
- Mutert, E., Fairhurst, T.H., von Uexküll, H.R., 1999. Agronomic management of oil palms on deep peat. *Better Crops Int.* 13, 22–27.
- Nelson, P.N., Banabas, M., Scotter, D.R., Webb, M.J., 2006. Using soil water depletion to measure spatial distribution of root activity in oil palm (*Elais guineensis* Jacq.) plantations. *Plant Soil* 286, 109–121.
- Nelson, P.N., Banabas, M., Goodrick, I., Webb, M.J., Huth, N.I., O'Grady, D., 2015. Soil sampling in oil palm plantations: a practical design that accounts for lateral variability at the tree scale. *Plant Soil* 394, 421–429.
- Novita, N., Kauffman, J.B., Hergoualc'h, K., Murdiyarso, D., Tryanto, D.H., Jupesta, J., 2021. Carbon stocks from peat swamp forest and oil palm plantation in Central Kalimantan, Indonesia. In: Djalante, R., Jupesta, J., Aldrian, E. (Eds.), *Climate Change Research, Policy and Actions in Indonesia*. Springer International Publishing, pp. 203–227.
- Oktarita, S., Hergoualc'h, K., Anwar, S., Verchot, L.V., 2017. Substantial N₂O emissions from peat decomposition and N fertilization in an oil palm plantation exacerbated by hotspots. *Environ. Res. Lett.* 12, 104007.
- Pardon, L., Bessou, C., Nelson, P.N., Dubos, B., Ollivier, Marichal, R., et al., 2016. Key unknowns in nitrogen budget for oil palm plantations: a review. *Agron. Sustain. Dev.* 36, 1–12.
- Pärm, J., Verhoeven, J.T.A., Butterbach-Bahl, K., Dise, N.B., Ullah, S., Aasa, A., et al., 2018. Nitrogen-rich organic soils under warm well-drained conditions are global nitrous oxide emission hotspot. *Nat. Commun.* 9, 1135.
- Prananto, J.A., Minasny, B., Comeau, L.P., Rudiyanto, R., Grace, P., 2020. Drainage increases CO₂ and N₂O emissions from tropical peat soils. *Glob. Chang. Biol.* 26, 4583–4600.
- Rinne, J., Tuittila, E.S., Peltola, O., Li, X., Raivonen, M., Alekseychik, P., et al., 2018. Temporal variation of ecosystem scale methane emission from a boreal fen in relation to temperature, water table position, and carbon dioxide fluxes. *Glob. Biogeochem. Cycles* 32, 1087–1106.
- Rochette, P., Liang, B.C., Pelster, D., Bergeron, O., Lemke, R., Kroebel, R., et al., 2018. Soil nitrous oxide emissions from agricultural soils in Canada: exploring relationships with soil, crop and climatic variables. *Agric. Ecosyst. Environ.* 254, 69–81.
- Sa'adi, Z., Yaseen, Z.M., Muhammad, M.K.I., Iqbal, Z., 2022. On the prediction of methane fluxes from pristine tropical peatland in Sarawak: application of a denitrification-decomposition (DNDC) model. *Environ. Sci. Pollut. Res.* 29, 30724–30738.
- Sakata, R., Shimada, S., Arai, H., Yoshioka, N., Yoshioka, R., Aoki, H., et al., 2015. Effect of soil types and nitrogen fertilizer on nitrous oxide and carbon dioxide emissions in oil palm plantations. *Soil Sci. Plant Nutr.* 61, 48–60.
- Schoneveld, G.C., Ekowati, D., Andrianto, A., van der Haar, S., 2019. Modeling peat- and forestland conversion by oil palm smallholders in Indonesian Borneo. *Environ. Res. Lett.* 14, 014006.
- Shcherbak, I., Millara, N., Robertson, G.P., 2014. Global meta-analysis of the nonlinear response of soil nitrous oxide (N₂O) emissions to fertilizer nitrogen. *Proc. Natl. Acad. Sci.* 111 9199–1204.
- Smith, J.U., Smith, P., Addiscott, T., 1996. Quantitative methods to evaluate and compare soil organic matter (SOM) models. In: Powlson, D.S., Smith, P., Smith, J.U. (Eds.), *Evaluation of Soil Organic Matter Models*. Springer, Berlin, pp. 181–199.
- Swails, E., Jaye, D., Verchot, L., Hergoualc'h, K., Schirrmann, M., Borchard, N., et al., 2018. Will CO₂ emissions from drained tropical peatlands decline over time? Links between soil organic matter quality, nutrients, and C mineralization rates. *Ecosystems* 21, 868–885.
- Swails, E., Hertanti, D., Hergoualc'h, K., Verchot, L., Lawrence, D., 2019. The response of soil respiration to climatic drivers in undrained forest and drained oil palm plantations in an Indonesian peatland. *Biogeochemistry* 142, 37–51.
- Swails, E., Hergoualc'h, K., Verchot, L., Novita, N., Lawrence, D., 2021. Spatio-temporal variability of peat CH₄ and N₂O fluxes and their contribution to peat GHG budgets in Indonesian forests and oil palm plantations. *Front. Environ. Sci.* 9, 617828.
- Syahrinudin, 2005. The potential of oil palm and forest plantations for carbon sequestration on degraded land in Indonesia. In: Denich, M., Martius, C., Rodgers, C., van de Giesen, N., Vlek, P. (Eds.), *Ecology and Development Series No. 28*. Cuvillier Verlag, Göttingen.
- Taft, H.E., Cross, P.A., Hastings, A., Yeluripati, J., Jones, D.L., 2019. Estimating greenhouse gases emissions from horticultural peat soils using a DNDC modelling approach. *J. Environ. Manag.* 233, 681–694.
- Takakai, F., Morishita, T., Hashidoko, Y., Darung, U., Kuramochi, K., Dohong, S., et al., 2006. Effects of agricultural land-use change and forest fire on N₂O emission from tropical peatlands, Central Kalimantan, Indonesia. *Soil Sci. Plant Nutr.* 52, 662–674.
- Tan, L., Ge, Z., Zhou, X., Li, S., Xiuzhen, L., Tang, J., 2019. Conversion of coastal wetlands, riparian wetlands, and peatlands increases greenhouse gas emissions: a global meta-analysis. *Glob. Chang. Biol.* 26, 1638–1653.
- Tang, J., Zhuang, Q., Shannan, R.D., White, J.R., 2010. Quantifying wetlands methane emissions with process-based models of different complexities. *Biogeosciences* 7, 3817–3837.
- Toma, Y., Takakai, F., Darung, U., Kuramochi, K., Limin, S.H., Dohong, S., Hatano, R., 2011. Nitrous oxide emission derived from soil organic matter decomposition from tropical agricultural peat soil in Central Kalimantan, Indonesia. *Soil Sci. Plant Nutr.* 57, 436–451.
- Velthof, G.L., Rietra, R.P.J.J., 2018. Nitrous Oxide Emissions from Agricultural Soils. Wageningen Environmental Research, Wageningen Report 2921.
- Wakhid, N., Hirano, T., 2021. Contribution of CO₂ emission from litter decomposition in an oil palm plantation on tropical peatland. *IOP Conf. Ser.: Earth Environ. Sci.* 648, 012133.
- Warren, M., Frohling, S., Dai, Z., Kurnianto, S., 2017. Impacts of land use, restoration, and climate change on tropical peat carbon stocks in the twenty-first century: implications for climate mitigation. *Mitig. Adapt. Strateg. Glob. Chang.* 22, 1041–1061.
- Wright, E.L., Black, C.R., Cheesman, A.W., Drage, T., Large, D., Turner, B.K., Sjögersten, S., 2011. Contribution of subsurface peat to CO₂ and CH₄ fluxes in a neotropical peatland. *Glob. Chang. Biol.* 17, 2867–2881.
- Yan, G., Mu, C., Xing, Y., Wang, Q., 2018. Responses and mechanisms of soil greenhouse gas fluxes to changes in precipitation intensity and duration: a meta-analysis for global perspective. *Can. J. Soil Sci.* 98, 591–603.
- Yu, Z., Loisel, J., Brosseau, D.P., Beilman, D.W., Hunt, S.J., 2010. Global peatland dynamics since the Last Glacial Maximum. *Geophys. Res. Lett.* 37, L13402.
- Zhang, Y., Li, C., Trettin, C.C., Li, H., Sun, G., 2002. An integrated model of soil, hydrology, and vegetation for carbon dynamics in wetland ecosystems. *Glob. Biogeochem. Cycles* 16 9–1.